CONF-940933--26

INTERNATIONAL ATOMIC ENERGY AGENCY

FIFTEENTH INTERNATIONAL CONFERENCE ON PLASMA PHYSICS AND CONTROLLED NUCLEAR FUSION RESEARCH

Seville, Spain, 26 September – 1 October 1994

IAEA-CN-60/D-P-II-3

Energetic Particle Destabilization of Shear Alfvén Waves in Stellarators and Tokamaks

D. A. Spong, B. A. Carreras, C. L Hedrick, J-N. Leboeuf
Oak Ridge National Laboratory
P. O. Box 2009, Oak Ridge, TN 37831-8071

A. Weller
Max-Planck-Institut für Plasmaphysik, IPP-EURATOM-Association
D-85748 Garching, Germany

*Research sponsored by the Office of Fusion Energy, U.S. Department of Energy, under contract DE-AC05-84OR21400 with Martin Marietta Energy Systems, Inc.

DISCLAIMER

Portions of this document may be illegible in electronic image products. Images are produced from the best available original document.

IAEA-CN-60/D-P-II-3

Energetic Particle Destabilization of shear Alfvén Waves in Stellarators and Tokamaks

Abstract: An important issue for ignited devices is the resonant destabilization of shear Alfvén waves by energetic populations. These instabilities have been observed in a variety of toroidal plasma experiments in recent years., including: beam-destabilized toroidal Alfvén instabilities (TAE) in low magnetic field tokamaks, ICRF destabilized TAE's in higher field tokamaks, and global Alfvén instabilities (GAE) in low shear stellarators. In addition, excitation and study of these modes is a significant goal of the TFTR-DT program and a component of the ITER physics tasks. We have developed a gyrofluid model which includes the wave-particle resonances necessary to excite such instabilities. The TAE linear mode structure is calculated nonperturbatively, including many of the relevant damping mechanisms, such as: continuum damping, non-ideal effects (ion FLR and electron collisionality), and ion/electron Landau damping. This model has been applied to both linear and nonlinear regimes for a range of experimental cases using measured profiles.

1. Gyrofluid Model

In order to analyze both the linear [1] and nonlinear [2] phases of shear Alfvén instabilities within a unified approach, we have developed a gyrofluid model with Landau closure based on a two-pole approximation to the plasma dispersion relation. By construction, this includes the inverse Landau growth effects necessary to drive the otherwise stable toroidal and global Alfvén eigenmodes unstable. The linear model used for the background plasma and fields consists of an Ohm's law and vorticity equation, as given below.

$$\frac{\partial\tilde{\psi}}{\partial t} = \vec{\nabla}_{\parallel}\tilde{\phi} + \frac{T_e}{m_i\omega_{ci}^2}\left(i\frac{k_{\parallel}^2}{\omega}R_{ei}\right)_{imag.}\nabla_{\perp}^2\tilde{\psi} \tag{1}$$

$$\frac{\partial U}{\partial t} = -\vec{\nabla}_{\parallel}\left(\frac{\tilde{J}_{\varphi} + J_{\varphi,eq}}{B_{\varphi}}\right) + \left[\hat{e}_{\varphi}\times\vec{\nabla}\left(\frac{R}{B_{\varphi}}\right)\right]\bullet\vec{\nabla}\tilde{p}_{\alpha} + \omega_{real}\rho_i^{\,2}\nabla_{\perp}^2 U - \frac{c^2\beta_{avg}(S_{ei})_{imag.}}{8\pi\omega_{real}}\Omega_d^2(\phi) \tag{2}$$

Here $R_{ei}^{-1} = 1 + Y_{0e}/D_e + \tau_i^{-1}(1 + Y_{0i}/D_i)$, $\tau_i = T_i/T_e$, $D_j = 1 + (i\nu_j/\omega)Y_{0j}$,

$Y_{0j} = \xi_j Z(\zeta_j)$, $\xi_j = \omega/\sqrt{2}k_{\parallel}v_{th,j}$, $\zeta_j = (\omega + i\nu_j)\xi_j/\omega$, $\Omega_d \equiv (\hat{b}\times\vec{\nabla}B)\bullet\vec{\nabla}$

$Y_{1j} = \xi_j\,[\zeta_j + (0.5 + \zeta_j^2)Z(\zeta_j)]$, $Y_{2j} = \xi_j[1.5\zeta_j + \zeta_j^3 + (0.5 + \zeta_j^2 + \zeta_j^4)Z(\zeta_j)]$, and

$$S_{ei} = Y_{2e} + \tau_i Y_{2i} - i\frac{\nu_e}{\omega}\frac{Y_{1e}^2}{D_e} - i\frac{\nu_i}{\omega}\frac{Y_{1i}^2}{D_i} + R_{ie}\left(\frac{Y_{1e}}{D_e} - \frac{Y_{1i}}{D_i}\right)^2;$$

Here $2\pi\tilde{\psi}$, U, and $-\tilde{\phi}/B_0$ are the fluctuating poloidal magnetic flux, toroidal component of vorticity and electrostatic potential, respectively. The vorticity equation (2) includes a finite ion FLR term and Landau damping on the background ions and electrons. In order to model the global Alfvén instability, which is observed in rather collisional conditions on W7AS, ion and electron collisions are included in the Landau damping terms. These tend to broaden and reduce the maxima in the ion and electron resonances. The Ohm's law includes a generalized resistivity which takes into account both the usual collisional resistive effects as well as collisionless effects, consistent with the presence of a finite $E_{||}$. These nonideal collisionless effects arise due to the high frequency, non-resonant ($k_{||} \neq 0$) nature of the Alfvén modes and the resulting incomplete cancellation of $E_{||}$ by the thermal electrons. The fast ion species (denoted by subscript α) is described by the following two equations for its perturbed density ($\tilde{n}_\alpha$) and parallel velocity moments ($\tilde{V}_{||\alpha}$):

$$\frac{\partial \tilde{n}_\alpha}{\partial t} = \frac{n_{0\alpha} T_{0\alpha}}{M_\alpha \Omega_{c\alpha}} \left\{ n_{0\alpha}^{-1} \Omega_d(\tilde{n}_\alpha) + q_\alpha T_{0\alpha}^{-1} \left[\Omega_d(\tilde{\phi}) - L_{n\alpha}^{-1} \frac{1}{r} \frac{\partial \tilde{\phi}}{\partial \theta} \right] \right\} - n_{0\alpha} \nabla_{||}^{(0)} \tilde{V}_{||\alpha}, \tag{3}$$

$$\frac{\partial \tilde{V}_{||\alpha}}{\partial t} = \frac{T_{0\alpha}}{M_\alpha \Omega_{c\alpha}} \left[\Omega_d(\tilde{V}_{||\alpha}) - \frac{q_\alpha}{M_\alpha R L_{n\alpha}} \frac{1}{r} \frac{\partial \tilde{\psi}}{\partial \theta} \right] - \left(\frac{\pi}{2} \right)^{1/2} v_{T\alpha} \left| \nabla_{||}^{(0)} \right| \tilde{V}_{||\alpha} - \frac{v_{T\alpha}^2}{n_{0\alpha}} \nabla_{||}^{(0)} \tilde{n}_\alpha \tag{4}$$

Here $L_{n\alpha}^{-1} = n_{0\alpha}^{-1} dn_{0\alpha}/dr$; also, $n_{0\alpha}$, $T_{0\alpha}$, M_α, $\Omega_{c\alpha}$, q_α, and $v_{T\alpha}$ are the fast ion density, temperature, mass, cyclotron frequency, charge, and thermal velocity, respectively. The Landau resonance arises from the third term on the right-hand side of equation (4). This system of equations is solved as an initial value problem for the 3-D mode structure in a straight field line coordinate system based on a toroidal, finite β equilibrium.

2. Toroidal Alfvén Instabilities

TAE instabilities occur in the gaps induced by toroidicity when two adjacent cylindrical shear Alfvén continua cross [3]; they involve the coupling of at least two poloidal harmonics and have been driven in tokamaks both by neutral beams [4-5] and ICRF produced tails [6]. We also predict TAE's to be accessible in moderate shear stellarators (e.g., ATF) and in low shear stellarators above a minimum toroidal mode number (e.g., $n \geq 3$ in W7-AS); however, none have yet been observed. An important topic currently under investigation is whether Alfvén instabilities can be driven by alpha populations in the DT phase of TFTR [7]. In Fig. 1 we show growth rates vs. the peak β_α for n = 2, 3 and 4 TAE instabilities in a typical TFTR DT supershot (dashed curves, #76770). As can be seen, the thresholds are significantly above the achieved values of $\beta_\alpha(0)$. This is consistent with experimental observations showing a lack of any new TAE activity in DT operation [7,8]. One possible way to enhance the accessibility of alpha-driven TAE's is through increasing the q(0) value. This moves the radial location of the TAE gaps inward, and aligns them more closely with the location of the maximum alpha pressure gradient. The effect of such profile changes is shown by the solid curves in Fig. 1 where MSE-measured q profiles [9] of an enhanced q(0) TFTR case (#75963) are used. Higher growth rates and lower $\beta_\alpha(0)$ thresholds are obtained which fall within the β_α range already achieved in TFTR. Such techniques for destabilizing TAE's in the central region of a tokamak can also be of interest in future ignited devices for ash removal through q-profile control. An alternate way to lower TAE thresholds is to lower the ion temperature, thus decreasing ion Landau damping. In Fig. 2 predicted TAE thresholds and achieved $\beta_\alpha(0)$'s are shown for a TFTR discharge (#75932) where a helium-puff was used in order to transiently cool the ions. However, as indicated, the achieved $\beta_\alpha(0)$ remained subcritical for driving TAE instabilities.

3. Global Alfvén Instabilities

Global Alfvén instabilities exist as discrete roots below minima in the shear Alfvén continua ; they tend to be dominated by a single poloidal mode number and have a global mode structure. Our model predicts that GAE modes may be excited in tokamaks which have central, slightly negative low shear regions. An example is shown in Fig. 3 for TFTR parameters. Such modes may become especially likely in devices such as TPX and ITER where significant bootstrap currents can create weak negative shear regions which will be in the same location as the maximum pressure gradient in the fast ion population.

GAE modes have been observed in the W7AS stellarator experiment [10] which operates with low values of magnetic shear. Their phase velocity is somewhat lower than the TAE mode, allowing them to be excited for $< v_{beam} > / v_A(0) = 0.15$ to 0.4. Also, they are slightly off-resonant with the equilibrium magnetic field helicity ($k_{\|} \neq 0$). Even though the ideal MHD, $\beta = 0$ gaps close off as rational iotas enter the plasma, we observe peaks in the growth rates and minima in the real frequencies near rational iota values (Fig. 4); this is due to a discretization of the contunuum by the nonideal effects included in our model (i.e., ion FLR, resistivity, etc.) and the effect of the finite fast ion pressure. Since the instability also persists away from the rational iota values, it cannot be avoided simply by keeping iota in between the low order rationals. In W7AS the GAE instability is observed to disappear at high β; the gyrofluid model indicates a possible cause for this stabilization is the increased shear in the iota profile with increasing β, with somewhat lesser effects coming from increased Landau damping on the ambient plasma. An important issue for future higher shear, higher β stellarators is whether there will be a stable window between the disappearance of the GAE (due to increasing shear) and the onset of the TAE instability.

4. Nonlinear TAE/GAE Behavior

The nonlinear gyrofluid model has been applied to TAE and GAE instabilities on both TFTR and W7-AS. A Fourier analysis of the simulated edge magnetic fluctuations has been compared with experiments and shows reasonably good agreement with measured spectra. An example of such a time-evolving frequency spectrum for TFTR parameters is shown in Fig. 5. The spectra are typically dominated by a peak at the main TAE frequency with higher harmonic peaks generated nonlinearly as the instability saturates. In the early stages of the nonlinear evolution, the mode number spectrum is dominated by the toroidal mode numbers with the highest growth rates; as a saturated state is reached, the nonlinearly generated n = 0 component typically dominates. This component results in profile modifications and $\vec{E} \times \vec{B}$ flow velocities. The saturation mechanisms have been analyzed [2], indicating that sheared velocity flow amplification and q-profile modification (through magnetic island formation) are the essential components necessary to achieve a saturated nonlinear state . This suggests a possible way of controlling the TAE using RF generated flows [11].

5. Conclusions

A gyrofluid model using Landau closure has proven to be a powerful technique for analyzing fast ion destabilized shear Alfvén instabilities such as the TAE and GAE. Applying this both to tokamaks and the low shear stellerator W7-AS we find that both types of modes can exist in either device under the appropriate conditions. The model has predicted that the typical TFTR DT supershot should be below the β_α threshold for alpha-driven TAE instabilities, but if q-profiles with higher q(0)'s can be generated, this threshold can be substantially reduced into a range of β_α that has been realized experimentally. Finally, the gyrofluid model has indicated that the TAE can achieve nonlinear saturation through mechanisms such as amplification of sheared flow velocities and quasilinear modification of the q-profile.

Acknowledgements

We would like to express our thanks to both the TFTR and W7-AS experimental and modeling groups for providing access to profile data we have used in our calculations. This research was sponsored by the Office of Fusion Energy, U.S. Department of Energy, under contract DE-AC05-84OR21400 with Martin Marietta Energy Systems, Inc.

References:

[1] D. A. SPONG, B. A. CARRERAS, C. L. HEDRICK, Phys. Fl. B **4**, 3316 (1992).

[2] D. A. SPONG, B. A. CARRERAS, C. L. HEDRICK, Phys. Plasmas **1** (5), 1994.

[3] C. Z. CHENG, L. CHEN, AND M. S. CHANCE, Ann. Phys. **161**, 21 (1985); C. Z. Cheng and M. S. Chance, Phys. Fluids **29**, 3695 (1986); G. Y. Fu and J. W. Van Dam, Phys. Fluids B **1**, 1949 (1989).

[4] K. L. WONG, R. J. FONCK, S. F. PAUL, D. R. ROBERTS, E. D. FREDRICKSON, R. NAZIKIAN, H. K. PARK, M. BELL, N. L. BRETZ, R. BUDNY, S. COHEN, G. W. HAMMETT, F. C. JOBES, D. M. MEADE, S. S. MEDLEY, D. MUELLER, Y. NAGAYAMA, D. K. OWENS, AND E. J. SYNAKOWSKI, Phys. Rev. Lett. **66,** 1874 (1991).

[5] W. W. HEIDBRINK, E. J. STRAIT, E. DOYLE, G. SAGER, AND R. SNIDER, Nuc. Fusion **31**, 1635 (1992).

[6] J. R. WILSON, J. C. HOSEA, R. MAJESKI, C. K. PHILLIPS, J. H. ROGERS, G. SCHILLING, J. E. STEVENS, G. TAYLOR, AND THE TFTR GROUP, R. GOLDFINGER, D. J. HOFFMAN, M. MURAKAMI, D. RASMUSSEN, F. RIMINI, Bull. Am. Phys. Soc. **37**, 1380 (1992).

[7] J. D. STRACHAN, et al., Phys. Rev. Lett. Vol. 72, No. 22, (3526) 1994.

[8] FREDERICKSON, E., et al., IAEA-CN-60/A-2-II-5, these Proceedings.

[9] LEVINTON, F., Princeton Plasma Physics Lab., personal communication (1994).

[10] A. WELLER, D. A. SPONG, R. JAENICKE, A. LAZAROS, F. P. PENNINGSFELD, S. SATTLER, W7-AS TEAM AND NBI GROUP, Phys. Rev. Lett. **72** (1220) 1994.

[11] G. G. CRADOCK, P. H. DIAMOND, M. ONO, H. BIGLARI, Phys. Plasmas **1**, 1944 (1994).

Figure Captions

Fig. 1 - Growth rates for TAE instabilities in a TFTR DT supershot vs. the central β_α value for a typical DT supershot with low q(0) (dashed curves) and for a higher q(0) case (solid curves). The shaded rectangular region represents the range of achieved central β_α's.

Fig. 2 - Time dependence of n = 2, 3, and 4 TAE β_α thresholds along with the experimentally achieved β_α for a TFTR DT case where helium was in puff ed in to transiently cool the ions.

Fig. 3 - (a) two similar q-profiles in TFTR which result in (b) TAE and GAE instabilities.

Fig. 4 - Dependence of real frequencies (dashed curves) and growth rates (solid curves) of a n = 2 GAE instability in W7-AS on the edge iota as the iota profile is uniformly changed (here $\tau_{Hp} = R_0 / v_A(0)$).

Fig. 5 - Time evolving frequency spectrum of edge magnetic fluctuations in a nonlinear gyrofluid simulation of a TAE instability.

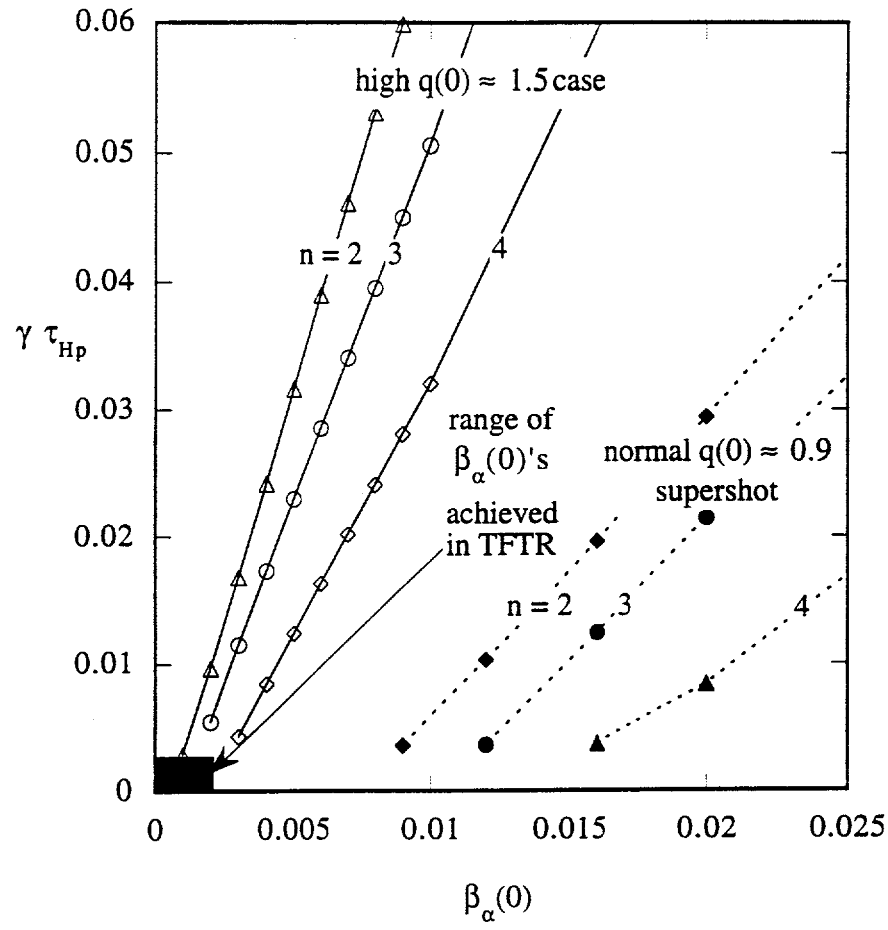

0.06
0.05
0.04
0.03
0.02
0.01
0
$\gamma\ \tau_{Hp}$
0
0.005
0.01
0.015
0.02
0.025
$\beta_\alpha(0)$
high q(0) ≈ 1.5 case
n = 2
3
4
range of
$\beta_\alpha(0)$'s
achieved
in TFTR
normal q(0) ≈ 0.9
supershot
n = 2
3
4

Figure 1

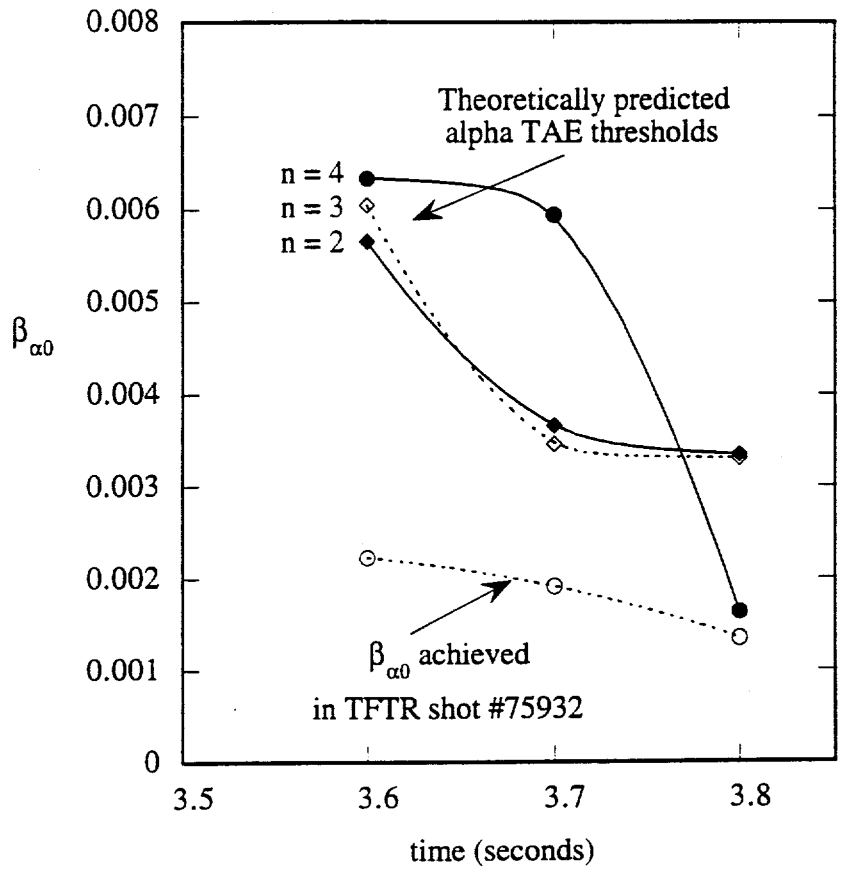
0.008
0.007
0.006
0.005
0.004
0.003
0.002
0.001
0
$\beta_{\alpha 0}$
Theoretically predicted
alpha TAE thresholds
n = 4
n = 3
n = 2
$\beta_{\alpha 0}$ achieved
in TFTR shot #75932
3.5
3.6
3.7
3.8
time (seconds)

Figure 2

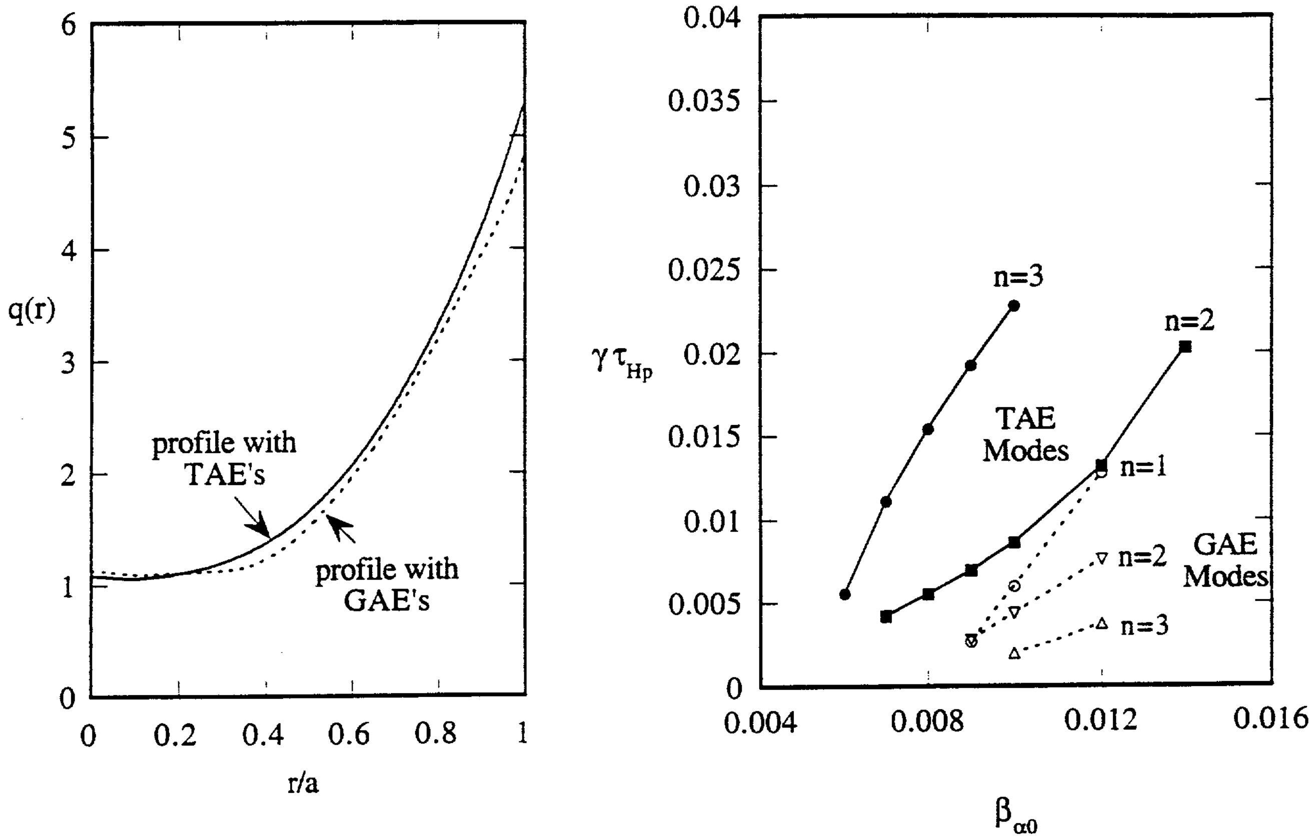
6
5
4
3
2
1
0
q(r)
0
0.2
0.4
0.6
0.8
1
r/a
profile with TAE's
profile with GAE's
0.04
0.035
0.03
0.025
0.02
0.015
0.01
0.005
0
γ τ_Hp
0.004
0.008
0.012
0.016
β_α0
n=3
n=2
TAE Modes
n=1
GAE Modes
n=2
n=3

Figure 3

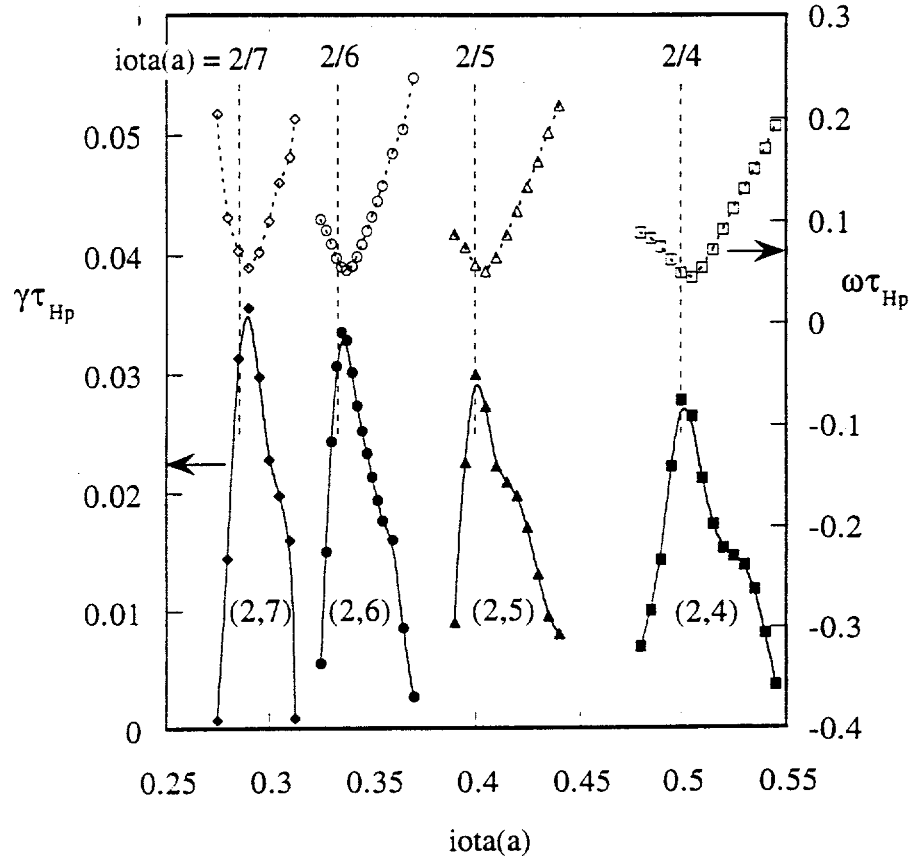
iota(a) = 2/7
2/6
2/5
2/4
0.05
0.04
0.03
0.02
0.01
0
$\gamma\tau_{Hp}$
0.3
0.2
0.1
0
-0.1
-0.2
-0.3
-0.4
$\omega\tau_{Hp}$
(2,7)
(2,6)
(2,5)
(2,4)
0.25
0.3
0.35
0.4
0.45
0.5
0.55
iota(a)

Figure 4

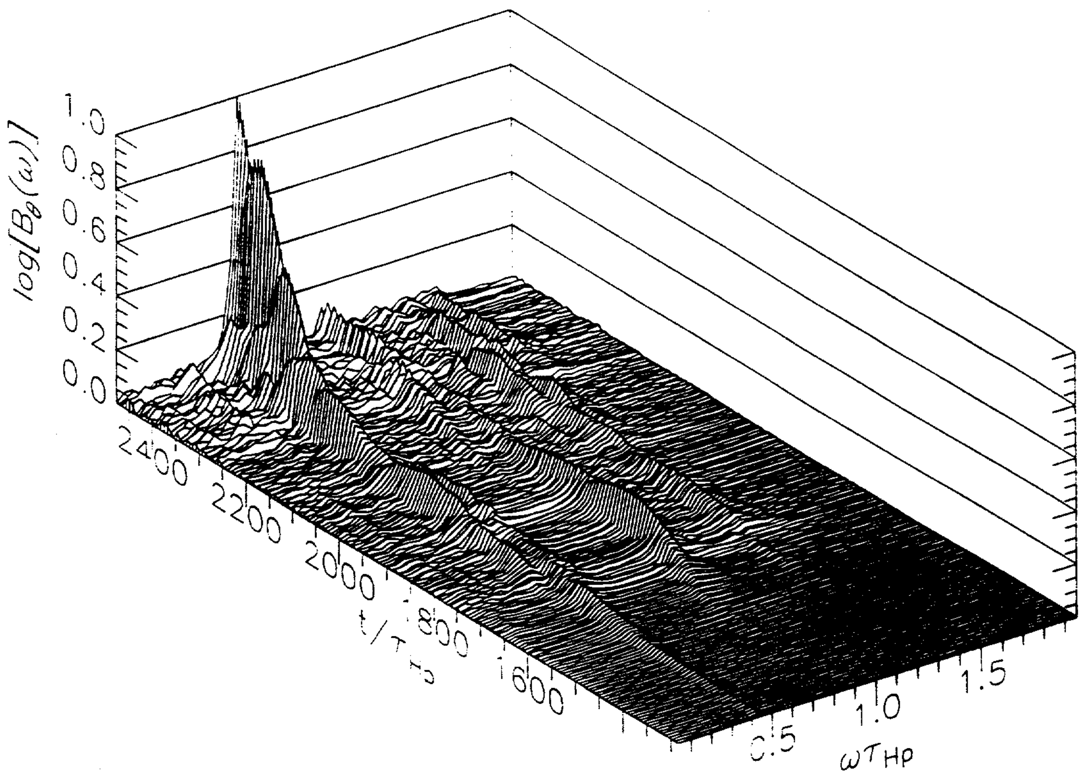

log[$B_\theta(\omega)$]
1.0
0.8
0.6
0.4
0.2
0.0
2400
2200
2000
1800
1600
t/τ_{Hp}
0.5
1.0
1.5
$\omega\tau_{Hp}$

Figure 5

IAEA-CN-60/D-P-II-3

Energetic Particle Destabilization of Shear Alfvén Waves in Stellarators and Tokamaks

D. A. Spong, B. A. Carreras, C. L Hedrick, J-N. Leboeuf
Oak Ridge National Laboratory
P. O. Box 2009, Oak Ridge, TN 37831-8071

A. Weller
Max-Planck-Institut für Plasmaphysik, IPP-EURATOM-Association
D-85748 Garching, Germany

*Research sponsored by the Office of Fusion Energy, U.S. Department of Energy, under contract DE-AC05-84OR21400 with Martin Marietta Energy Systems, Inc.

Introduction and Motivations

- Discrete Shear Alfvén modes exist within gaps of the ideal MHD continua (see next plot)
- Can be resonantly destabilized by fast ions
  - » $(\omega/k_{||})_{gap} \approx v_{fast,ion}$
  - » Fusion alphas, Neutral beam heating, RF Minority tails
- Resonant excitation → resonant loss
  - » unacceptable localized heat deposition on first wall
  - » lowered heating efficiency
- Alfvén instabilities are inherently damped
  - » Continuum absorption, ion/electron Landau, ion FLR, etc.
  - » Theoretical modeling/experiment can help identify stable regimes

Features of TAE/GAE Gyrofluid Model:

- Non-perturbative approach
- Inherently includes continuum damping and multiple gap structures
- Other damping included: ion/electron Landau, ion FLR, resistivity, electron collisional effects
- Calculates global radial structure - sensitive to profile effects (uses TRANSP results)
- Applicable both linearly and nonlinearly

MAGNETIC FIELD GEOMETRIES:

TFTR

W7-AS

TFTR Flux Surface with Magnetic Field Lines

Color shading indicates TAE mode structure

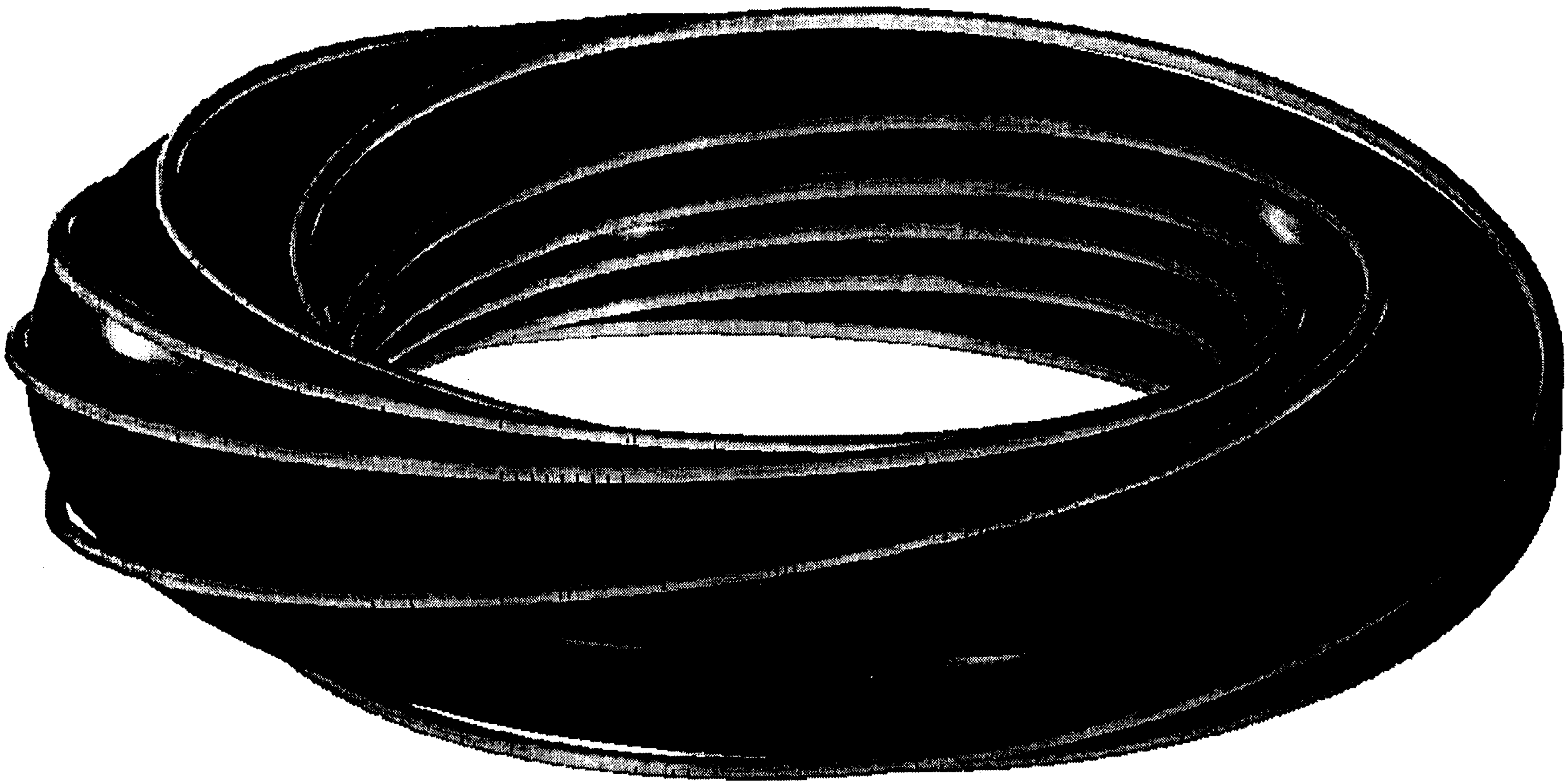

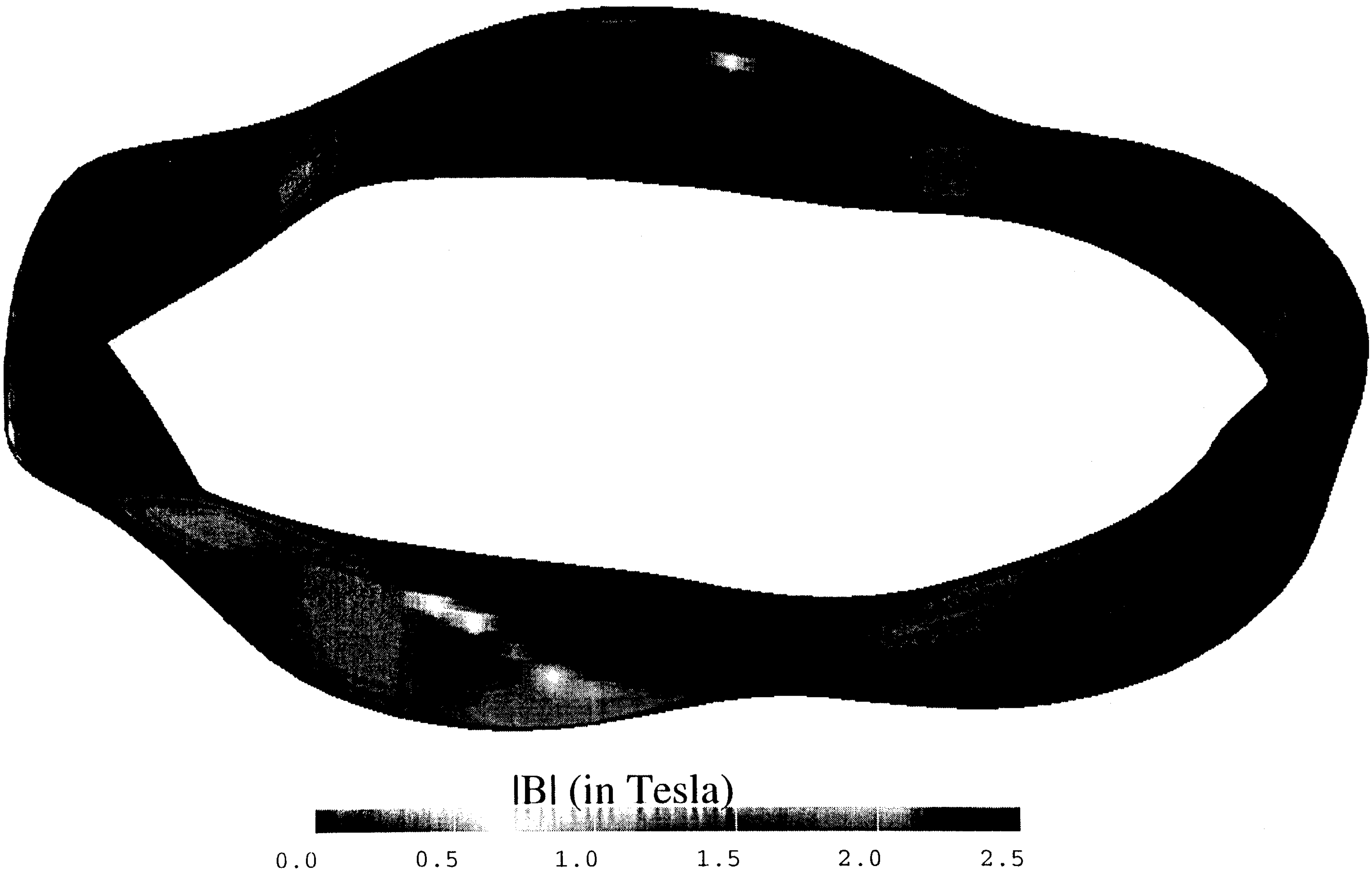
|B| (in Tesla)
0.0
0.5
1.0
1.5
2.0
2.5

METHODS USED:

- Our model consists of a four-field set of gyrofluid time evolution equations
- These are solved in toroidal geometry for the full 3-D mode structure
- A modified version (TAE/FL) of the FAR initial value code is used.
- References:

  - » L. Charlton, J. A. Holmes, H. R. Hicks, V. E. Lynch, and B. A. Carreras, J. Comput. Phys. 63, 107 (1986).
  - » D. A. Spong, B. A. Carreras, C. L. Hedrick, Phys. Fl. B 4, 3316 (1992).
  - » D. A. Spong, B. A. Carreras, C. L. Hedrick, Phys. Fl. B 4, 3316 (1992).
  - » D. A. Spong, B. A. Carreras, C. L. Hedrick, Phys. Plasmas 1 (5), 1994.

(1) A generalized Ohm's law

This includes: (a) the usual collisional resistivity and (b) a collisionless resistivity caused by incomplete cancellation of $E_{||}$ by the electrons for $k_{||} \neq 0$ modes at Alfvénic frequencies.

$$\boxed{\frac{\partial \tilde{\psi}}{\partial t} = \vec{\nabla}_{\parallel}\tilde{\phi} + \frac{n_e e^2}{m_i \omega_{ci}^2} \mathrm{Imag}(\eta_G) \nabla_{\perp}^2 \tilde{\psi}}$$

where $\eta_G = i \dfrac{k_{\parallel}^2 T_e}{\omega n_e e^2} R_{ei}$; $\quad R_{ei}^{-1} = 1 + \dfrac{Y_{0e}}{D_e} + \tau_i^{-1}\left(1 + \dfrac{Y_{0i}}{D_i}\right)$; $\quad \tau_i = \dfrac{T_i}{T_e}$

$Y_{0j} = \xi_j Z(\zeta_j)$; $\quad D_j = 1 + \dfrac{i\nu_j}{\omega} Y_{0j}$; $\quad \xi_j = \dfrac{\omega}{\sqrt{2} k_{\parallel} v_{th,j}}$; $\quad \zeta_j = \dfrac{\omega + i\nu_j}{\omega} \xi_j$

Asymptotic limits:

$$\frac{n_e e^2}{m_i \omega_{ci}^2} \mathrm{Imag.}(\eta_G) = \begin{cases} \left(\sqrt{\dfrac{\pi}{2}} \dfrac{\rho_{ion}^2}{\tau_i} \dfrac{v_A^2}{v_{th,e}} |\nabla_{\parallel}|\right) & \text{for } \nu_e / \omega << 1 \\ \left(\dfrac{m_e \nu_e}{2 n_e e^2}\right) & \text{for } \nu_e / \omega >> 1 \end{cases}$$

(2) Toroidal component of vorticity

includes electron and ion Landau damping (with collisional effects) and ion FLR:

$$\boxed{\frac{\partial U}{\partial t} = -\vec{v}_\perp \cdot \vec{\nabla} U - \vec{\nabla}_\parallel \left(\frac{\tilde{J}_\varphi + J_{\varphi,eq}}{B_\varphi} \right) + \left[\hat{e}_\varphi \times \vec{\nabla} \left(\frac{R}{B_\varphi} \right) \right] \bullet \vec{\nabla} \tilde{p}_\alpha + \omega_{real} \rho_i{}^2 \nabla_\perp^2 U - \frac{c^2 \beta_{avg} \, \mathrm{Imag}(S_{ei})}{8\pi \omega_{real}} \Omega_d^2(\phi)}$$

where $S_{ei} = Y_{2e} + \tau_i Y_{2i} - i \frac{\nu_e}{\omega} \frac{Y_{1e}^2}{D_e} - i \frac{\nu_i}{\omega} \frac{Y_{1i}^2}{D_i} + R_{ie} \left(\frac{Y_{1e}}{D_e} - \frac{Y_{1i}}{D_i} \right)^2$

$$Y_{0j} = \xi_j \, Z(\zeta_j); \qquad Y_{1j} = \xi_j \left[\zeta_j + \left(\frac{1}{2} + \zeta_j^2 \right) Z(\zeta_j) \right];$$

$$Y_{2j} = \xi_j \left[\frac{3}{2} \zeta_j + \zeta_j^3 + \left(\frac{1}{2} + \zeta_j^2 + \zeta_j^4 \right) Z(\zeta_j) \right]$$

$$\xi_j = \frac{\omega}{\sqrt{2} k_\parallel v_{th,j}}; \qquad \zeta_j = \frac{\omega + i\nu_j}{\omega} \xi_j$$

(3) Fast ion gyrofluid equations with Landau closure (two-pole approximation):

$$\frac{\partial \tilde{n}_\alpha}{\partial t} = \omega_{d\alpha}\mathbf{\Omega}_d(\tilde{n}_\alpha) - n_{0\alpha}\nabla_\parallel^{(0)}\tilde{v}_{\parallel\alpha} + n_{0\alpha}\mathbf{\Omega}_d(\phi) - \frac{dn_{0\alpha}}{dr}\frac{1}{r}\frac{\partial\phi}{\partial\theta} + \overline{D}_{p_\alpha}\nabla_{\perp 0}^2\tilde{n}_\alpha$$

$$\frac{\partial \tilde{v}_{\parallel\alpha}}{\partial t} = \omega_{d\alpha}\mathbf{\Omega}_d(\tilde{v}_{\parallel\alpha}) - \left(\frac{\pi}{2}\right)^{1/2} v_{th\alpha}|\nabla_\parallel^{(0)}|\tilde{v}_{\parallel\alpha} - \frac{v_{th\alpha}^2}{n_{0\alpha}}\nabla_\parallel^{(0)}\tilde{n}_\alpha - \frac{v_{th\alpha}^2}{n_{0\alpha}}\frac{dn_{0\alpha}}{dr}\frac{1}{r}\frac{\partial\psi}{\partial\theta} + \overline{D}_{v_{\parallel\alpha}}\nabla_{\perp 0}^2\tilde{v}_{\parallel\alpha},$$

where $\mathbf{\Omega}_d$ is the operator:

$$\mathbf{\Omega}_d \equiv \frac{R^2}{2}\frac{\partial}{\partial r}\left(\frac{1}{R^2}\right)\frac{1}{r}\frac{\partial}{\partial\theta} - \frac{R^2}{2r}\frac{\partial}{\partial\theta}\left(\frac{1}{R^2}\right)\frac{\partial}{\partial r} \propto (\hat{b}\times\nabla B)\bullet\nabla,$$

$$\omega_{c\alpha} = \Omega_{c\alpha}\tau_{Hp}, \quad v_{th\alpha} = (T_{0\alpha}/M_\alpha)^{1/2}/v_A(r=0),$$

These equations are solved using the TAE/FL initial value code

- Implicit linear/explicit nonlinear algorithm - extension of FAR code (L. Charlton, et al., J. Comput. Phys. 63, 107 (1986))
- Linearly, all growing modes can be identified
- Accepts general noncircular tokamak equilibria - uses straight field line coordinates
- 3-D mode structure is represented using Fourier expansions in ζ and θ, finite difference grid in radius

$$X(\rho,\theta,\zeta) = \sum_{mn}\left[X^{(c)}_{mn}(\rho)\cos(m\theta+n\zeta) + X^{(s)}_{mn}(\rho)\sin(m\theta+n\zeta)\right]$$

- Iteration scheme:

$$L\frac{\partial}{\partial t}\vec{X} = R\vec{X} \quad \Rightarrow \quad \vec{X}^{n+1} = \left[L - \frac{\Delta t}{2}R\right]^{-1}\left[L + \frac{\Delta t}{2}R\right]\vec{X}^{n}$$

ornl

TAE INSTABILITIES in TFTR-DT

Lower instability thresholds are required to observe alpha-driven TAE's in TFTR.

- **Alphas are relatively dilute: $\beta_\alpha(0) \leq 0.003$**
  - » Compare to $\beta(0)$ of beams and RF tails of ≈ 0.01
- **Minimization of TAE damping**
  - » Decrease T_{ion} to lower ion Landau damping
  - » Vary $q(r)$, $n_{ion}(r)$ to lower continuum damping
- **Enhancement of TAE instability drive**
  - » Increase $q(0)$ in order to align TAE gap structure with peak alpha pressure gradient
  - » Vary v_α/v_A to obtain stronger resonance coupling

Lowering T_{ion} decreases TAE thresholds

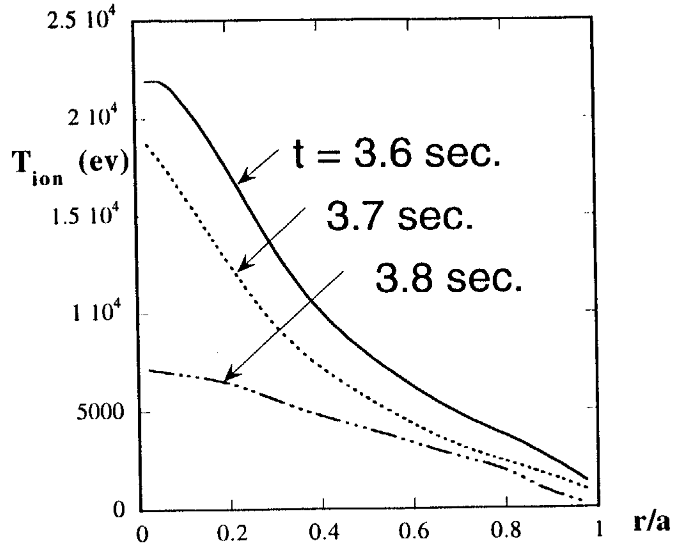

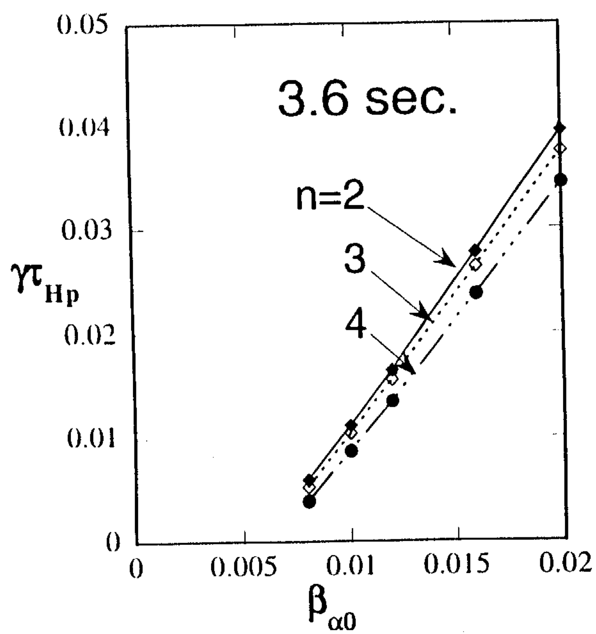

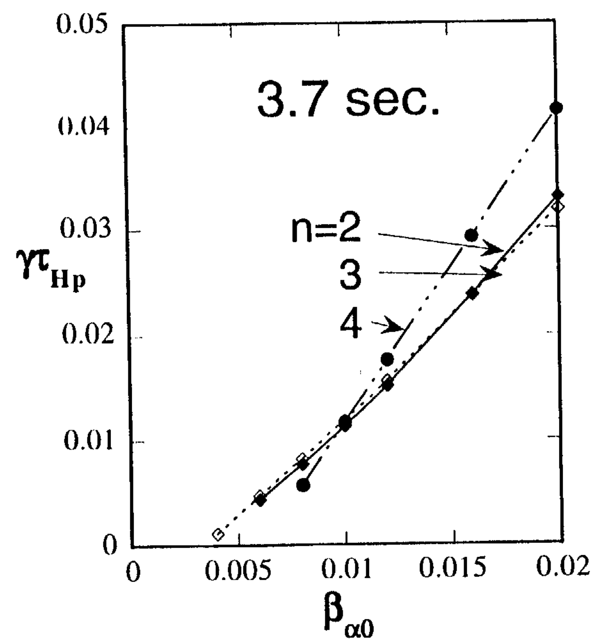

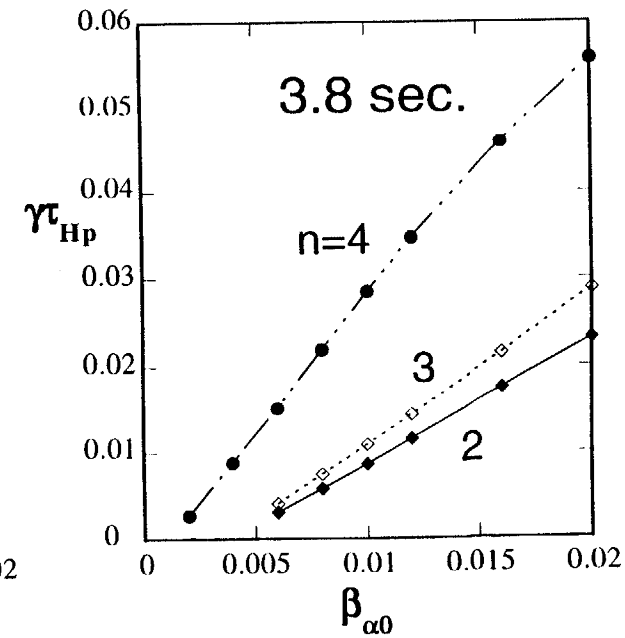

With lower T_{ion}, the alpha-driven TAE threshold is reduced, but the achieved β_α also decreases in time:

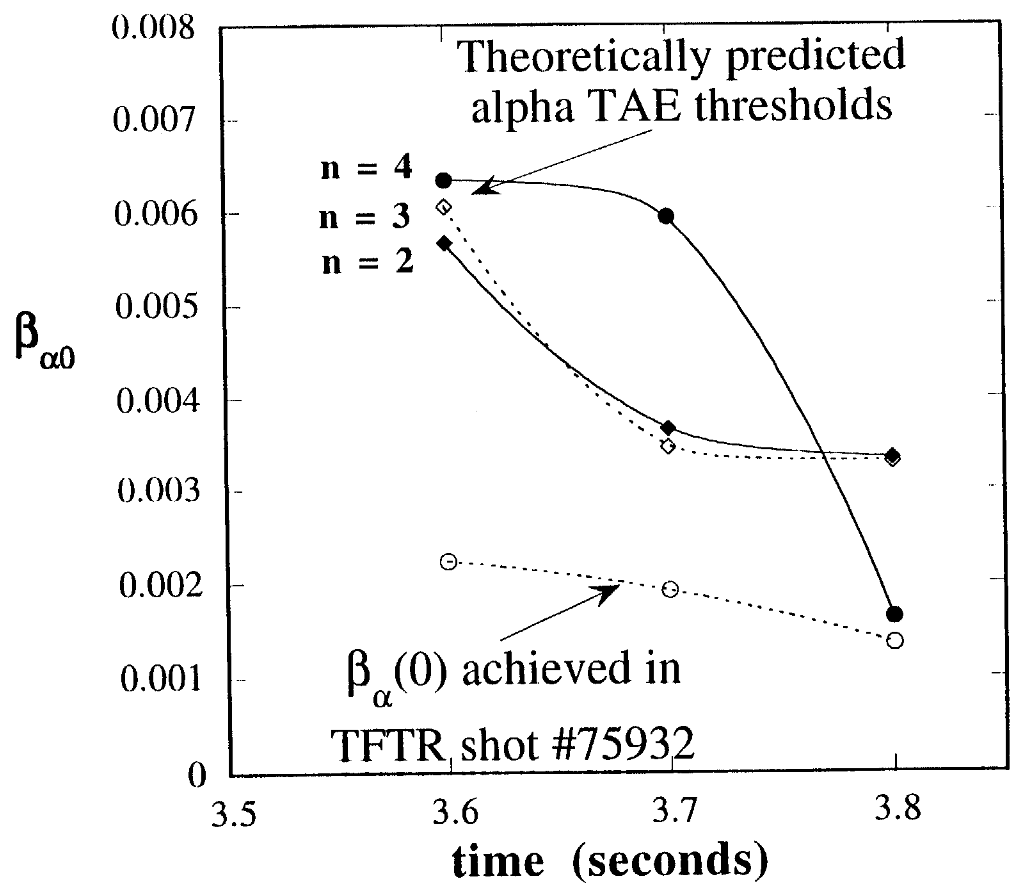

With increasing q(0) the TAE gap locations move inward, becoming more aligned with the peak in dp_α/dr.

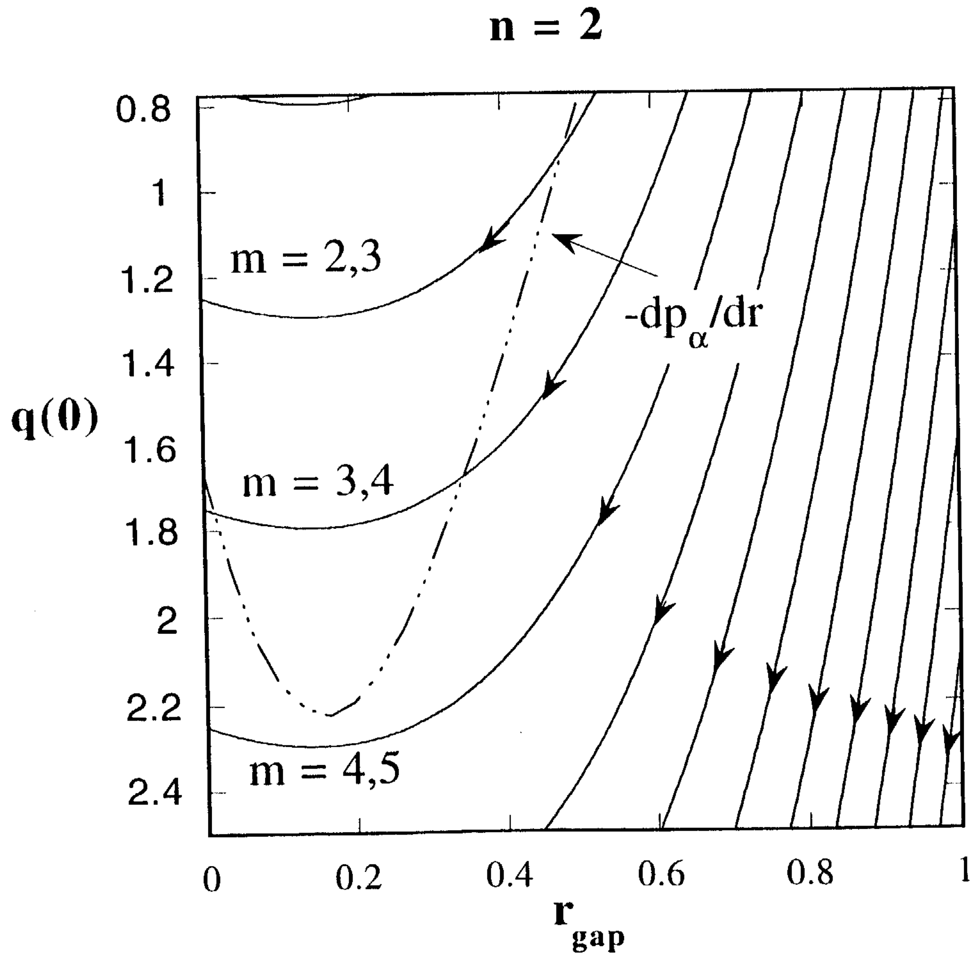

TFTR has obtained high q(0) cases in DD which would lead to lowered α TAE thresholds in DT.

MSE measured q profile evolution in shot#75963 (from Fred Levinton)

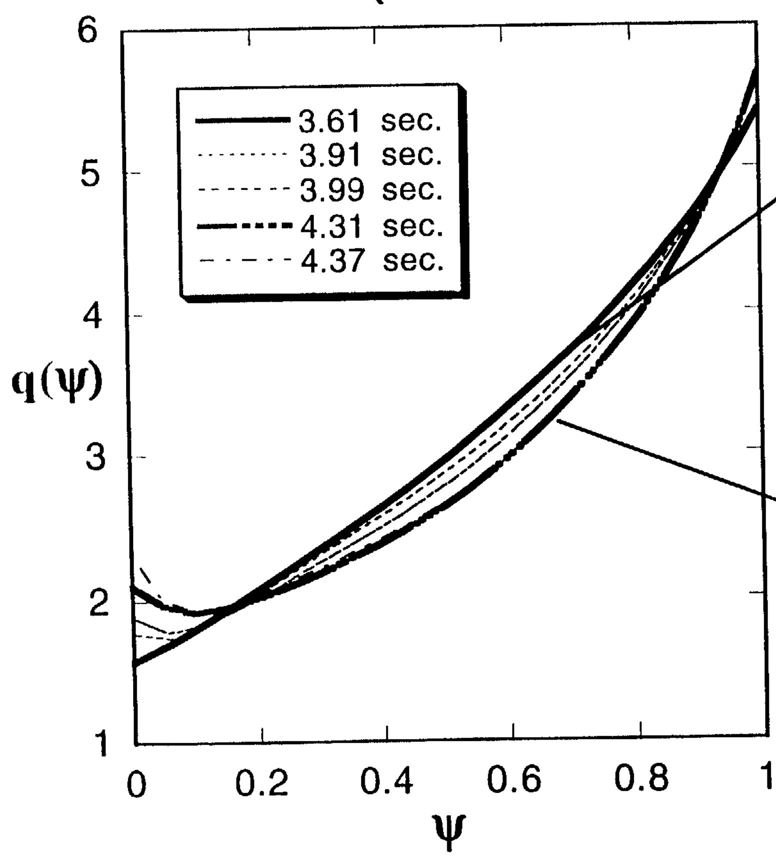

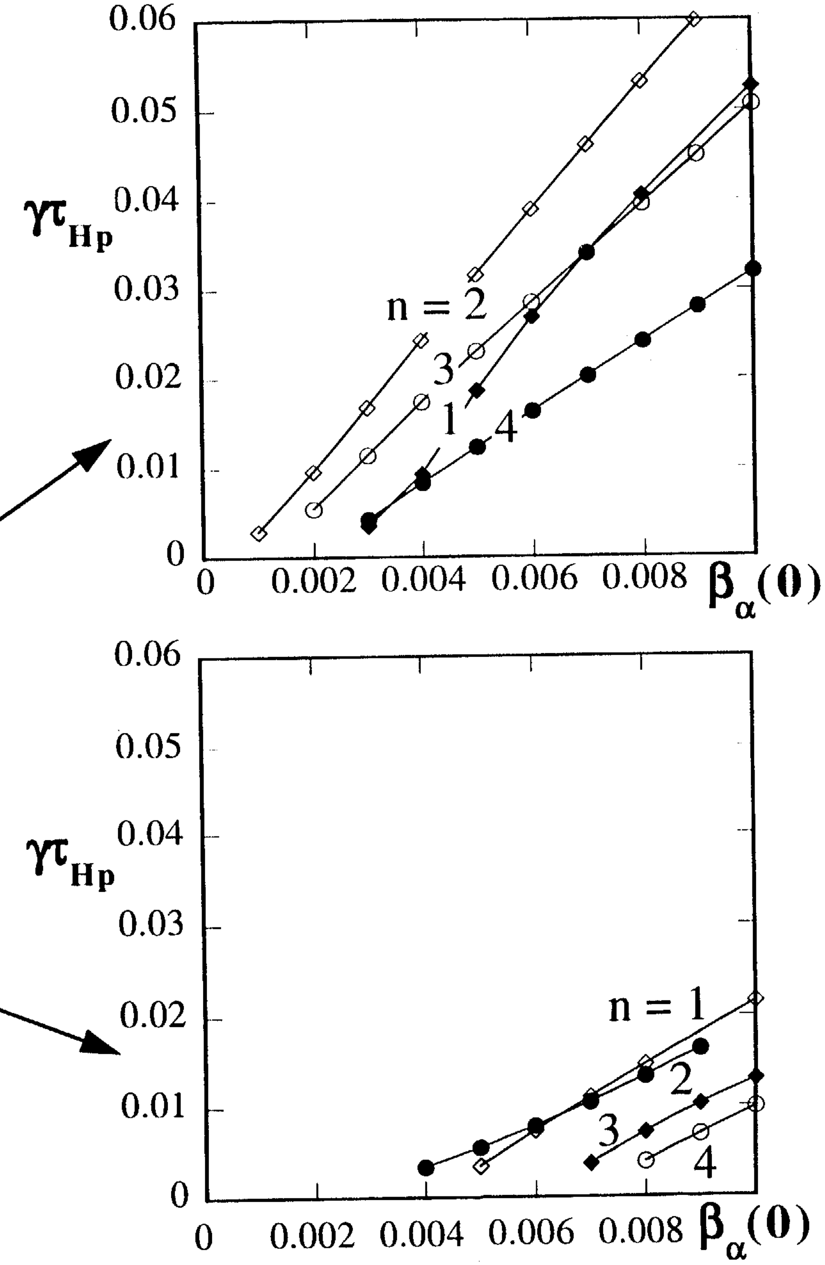

Comparison of a high q(0) TFTR case (#75963) with a typical supershot (#76770) shows significantly lowered TAE thresholds:

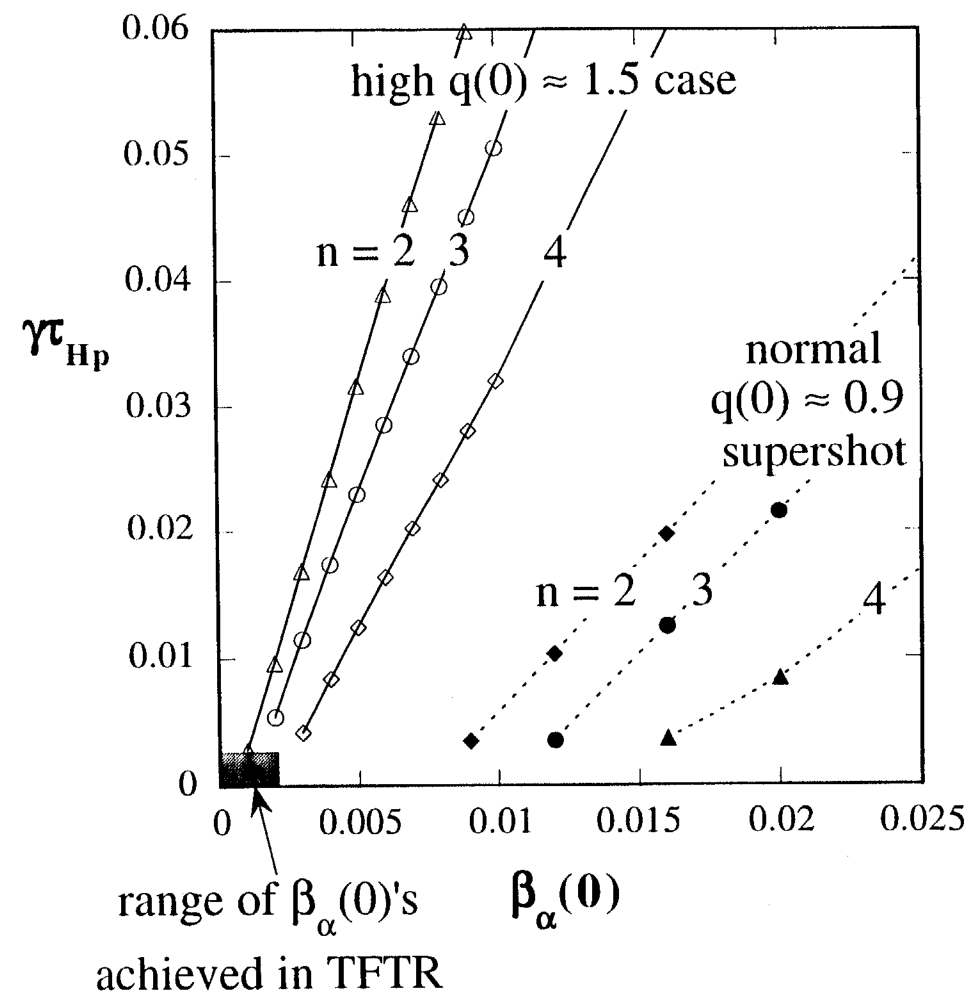

GAE INSTABILITIES in TOKAMAKS

With sufficiently flat q-profiles, tokamaks (TFTR) can also be unstable to GAE instabilities.

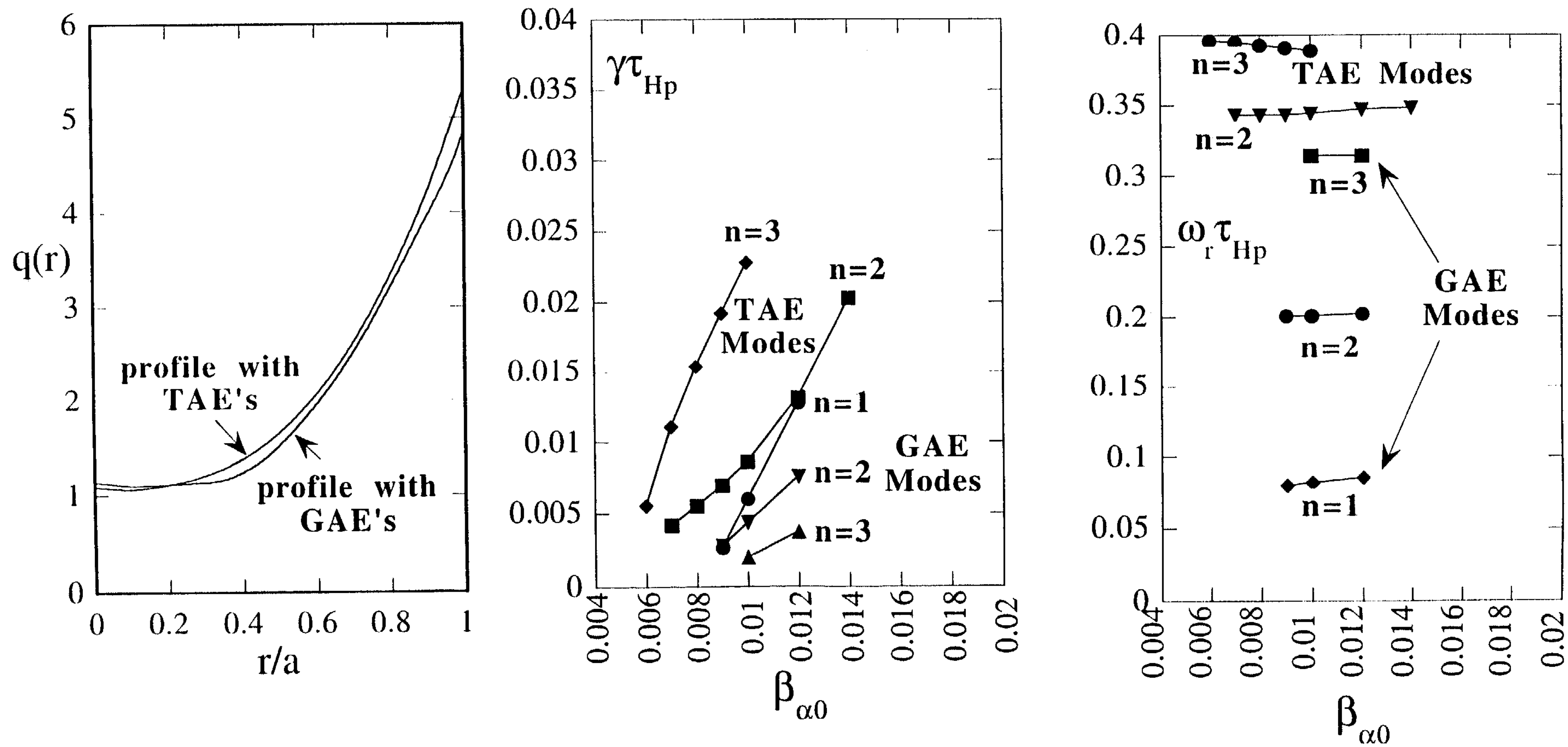

TAE density fluctuations should show more of a ballooning signature than those of the GAE:

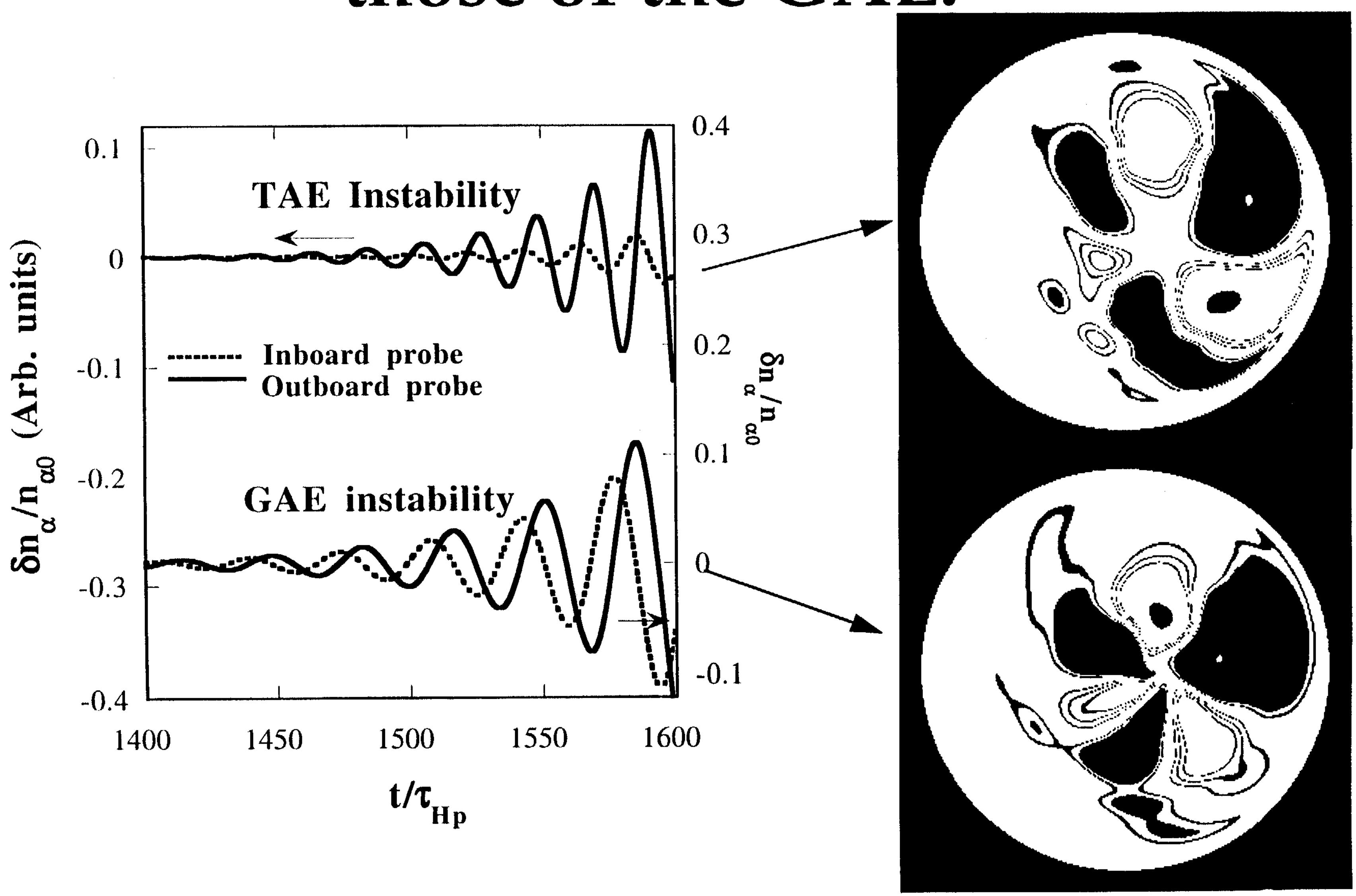

GAE INSTABILITIES in W7-AS

Global Alfvén Stability Issues in W7AS

- **Profile, parameter sensitivities**
  - » v_{beam}/v_A, $p_{beam}(r)$, $f_{beam}(E)$, β_{beam}
  - » iota(r), d(iota)/dr
- **What causes the GAE to appear/disappear?**
- **Relation between GAE and TAE modes**
  - » TAE's become possible at higher n's, v_{fast}/v_A, shear
  - » TAE's may be more relevant to α's in stellarators
- **How does one extend present GAE observations/physics to future devices?**
  - » Do GAE instabilities provide a means for ash removal?
  - » With somewhat larger shear will there be a stability window between the GAE and TAE modes?

For a typical W7AS low shear, iota > 1/3 profile, only the GAE is present at low n (= 1, 2). However, for n ≥ 3 both TAE and GAE modes coexist.

- For a TAE root to exist, there must be enough variation in q(r) such that

  $$\mathbf{k_{||,m} = -k_{||,m+1}} \text{ or } q(r) = (2m + 1)/2n$$

- With a q-profile of the form: $q(r) = m/n + \delta q$, this implies that $\boldsymbol{\delta q \geq 1/2n}$
- As n increases TAE roots become accessible.

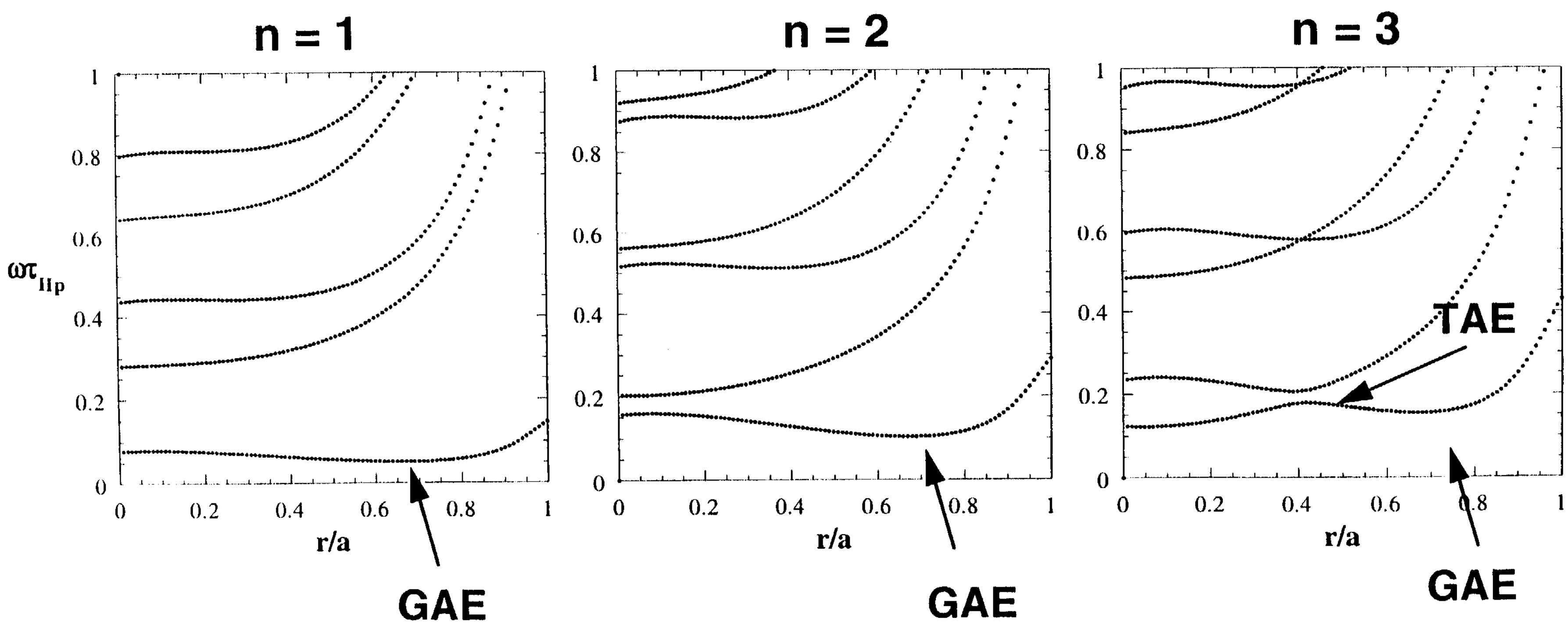

The GAE instability can be excited in low shear stellarators at relatively low values of v_{hot}/v_A.

W7AS #11474

(iota > 1/3)

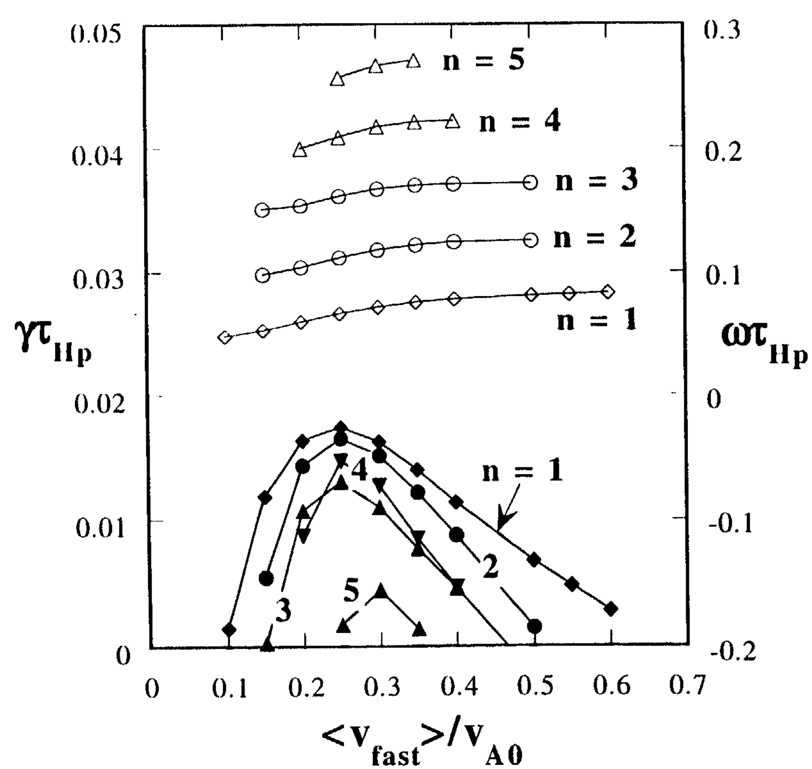

W7AS # 19657

(iota > 1/2)

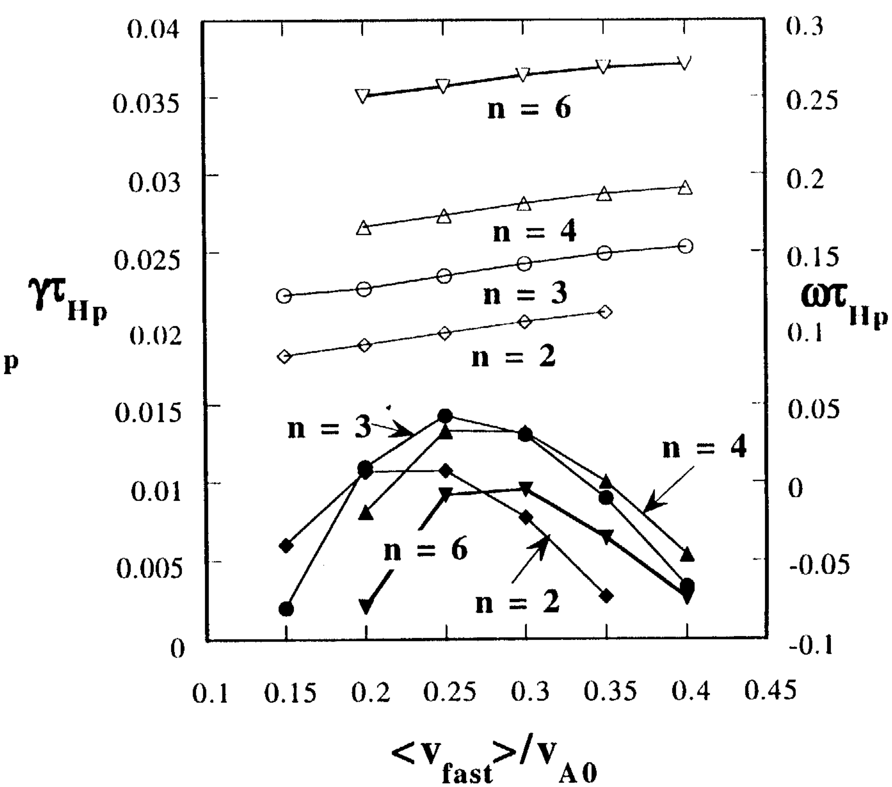

The following plots show the GAE 2-D mode structure for a W7-AS iota > 1/3 case vs. toroidal mode number:

$n = 1$

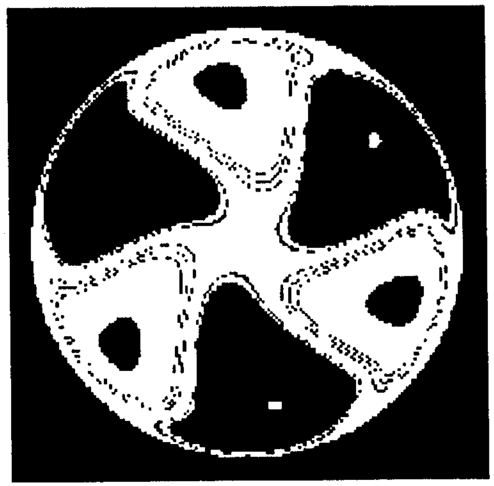

$n = 2$

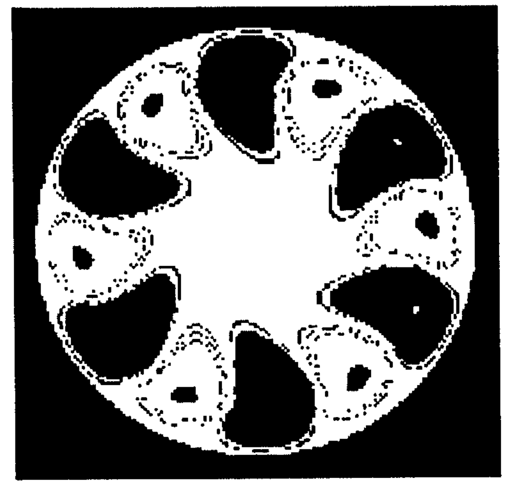

$n = 3$

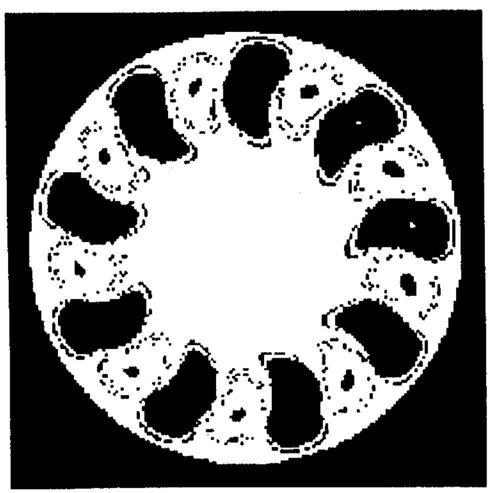

$n = 4$

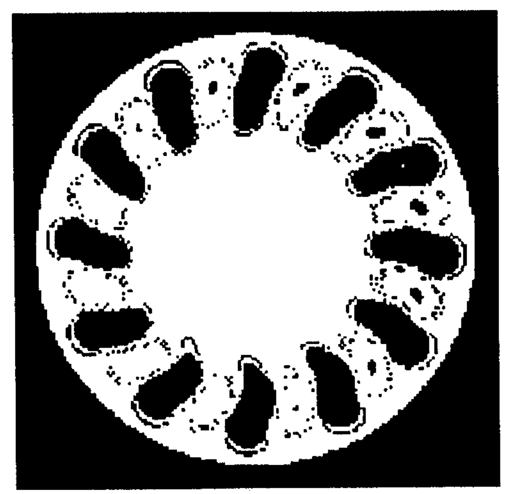

Scanning in iota(a) shows that, although the GAE mode is nonresonant, its growth is strongest when its helicity is aligned with that of the equilibrium field:

n = 1

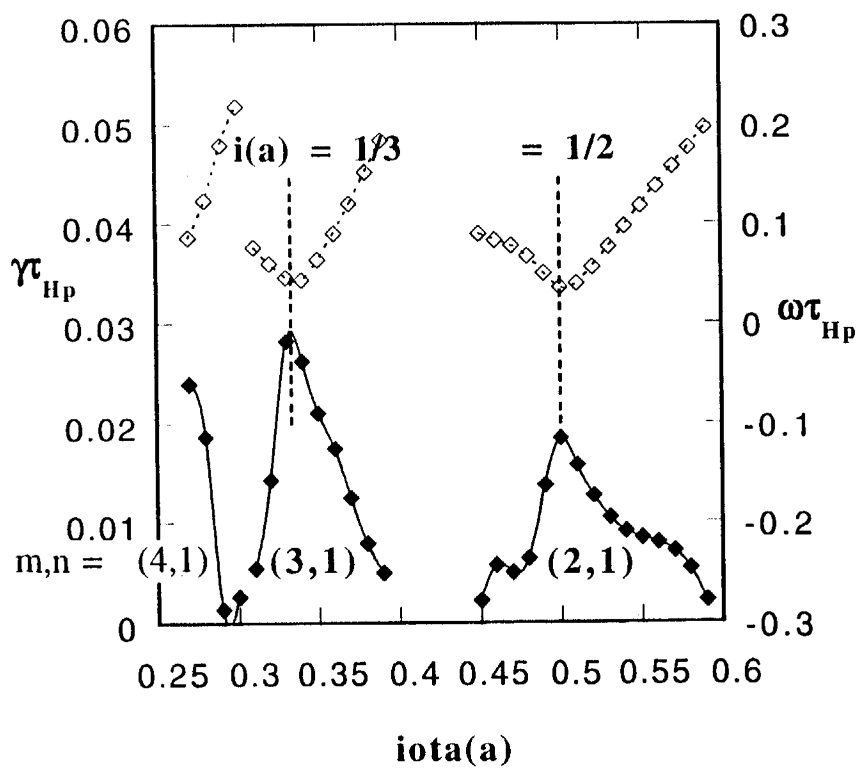

n = 2

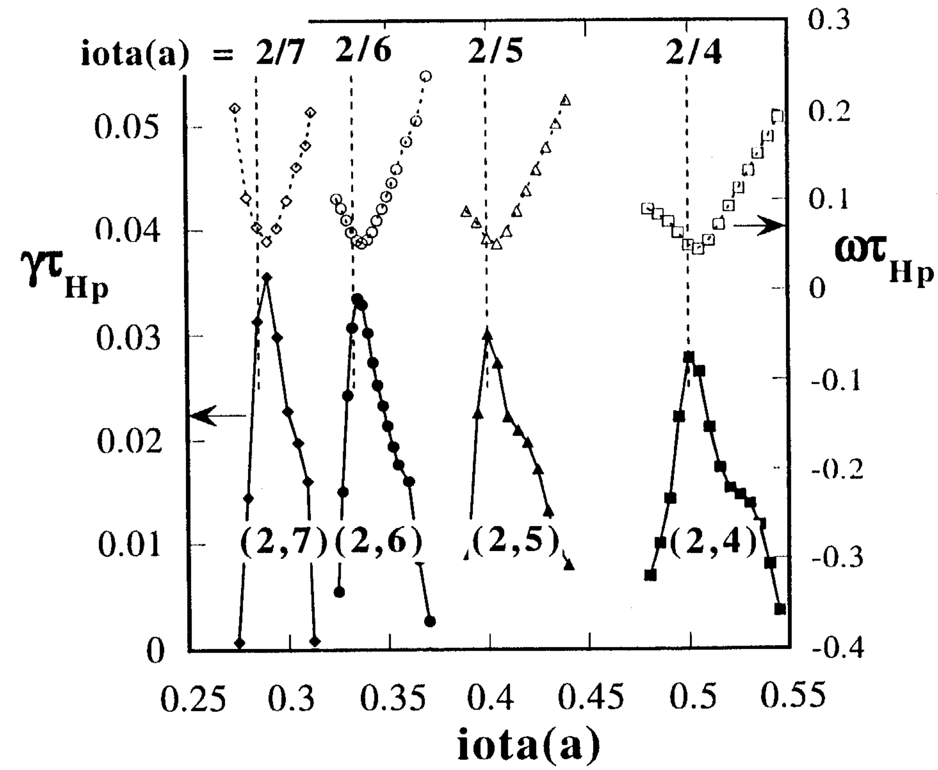

Slight increases in the shear of iota can stabilize the GAE instability:

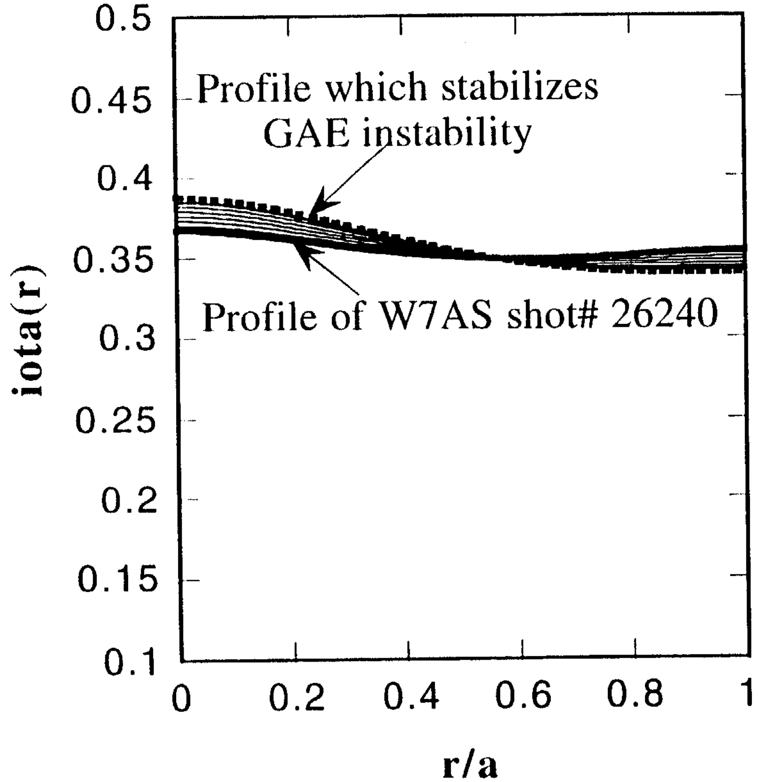

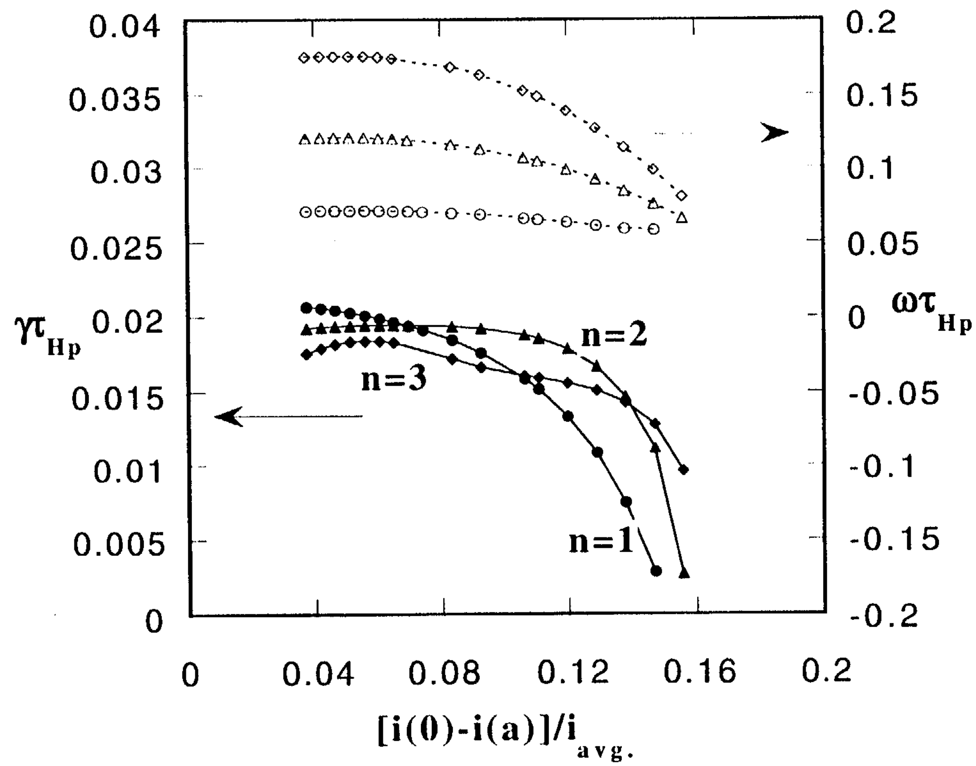

ornl

NONLINEAR EVOLUTION of TAE and GAE INSTABILITIES

- **Gyrofluid models offer relatively high radial and Fourier mode resolution**
  - » This is necessary to analyze saturation mechanisms such as:
    - Sheared flow generation/amplification
    - q-profile modification
    - Alpha density convection
    - Nonlinear frequency shifts and resonance detuning
  - » TAE's inherently involve mode couplings even in the linear phase. They become even more important nonlinearly
  - » Requirements for treating noncircular cross sections (e.g. ITER) are especially demanding
- **Nonlinear gyrofluid models are especially relevant to:**
  - » Higher magnetic field TAE regimes which often show steady state Alfvénic turbulence without measurable direct particle loss
  - » Larger, high current devices such as ITER where direct losses will be diminished and orbit width effects are smaller
- **It is important in the nonlinear evolution of the TAE to include $n = 0$ components of n_{fast}, ψ, ϕ, and $v_{||, fast}$. These are generated from the nonlinear beatings of the $n > 0$ modes.**

The nonlinear saturated state of the TAE mode involves extensive coupling in both m and n (i.e., poloidal and toroidal mode numbers)

Mode selection used:

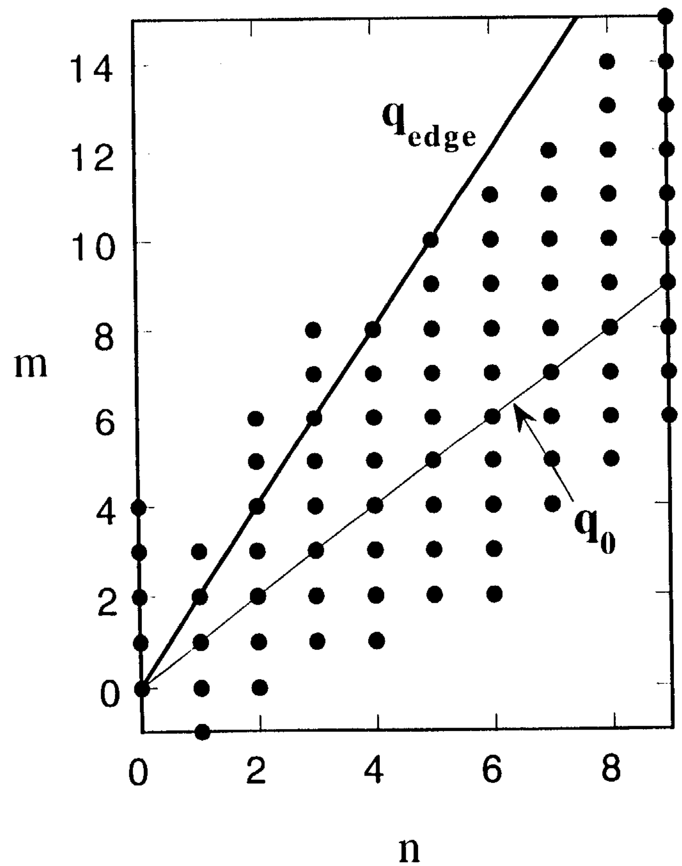

m, n spectrum at t = $1900\tau_{Hp}$

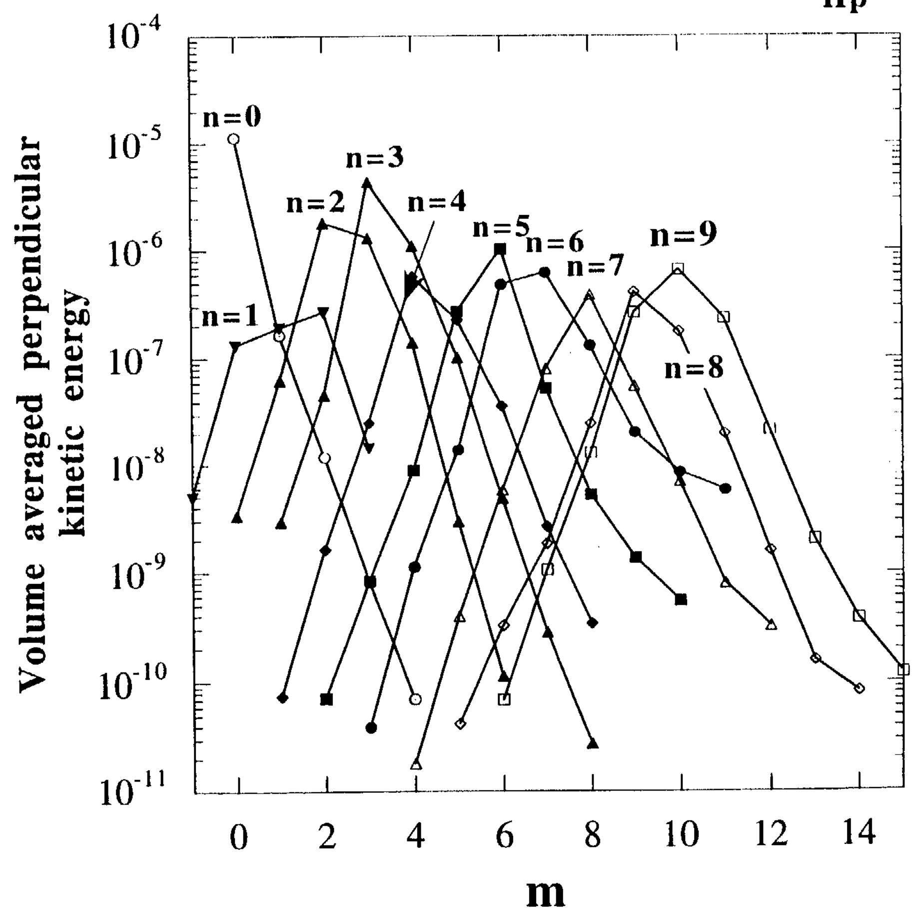

Evolution of R.M.S. and volume averaged quantities shows dominance of the n = 0 component in the nonlinear phase:

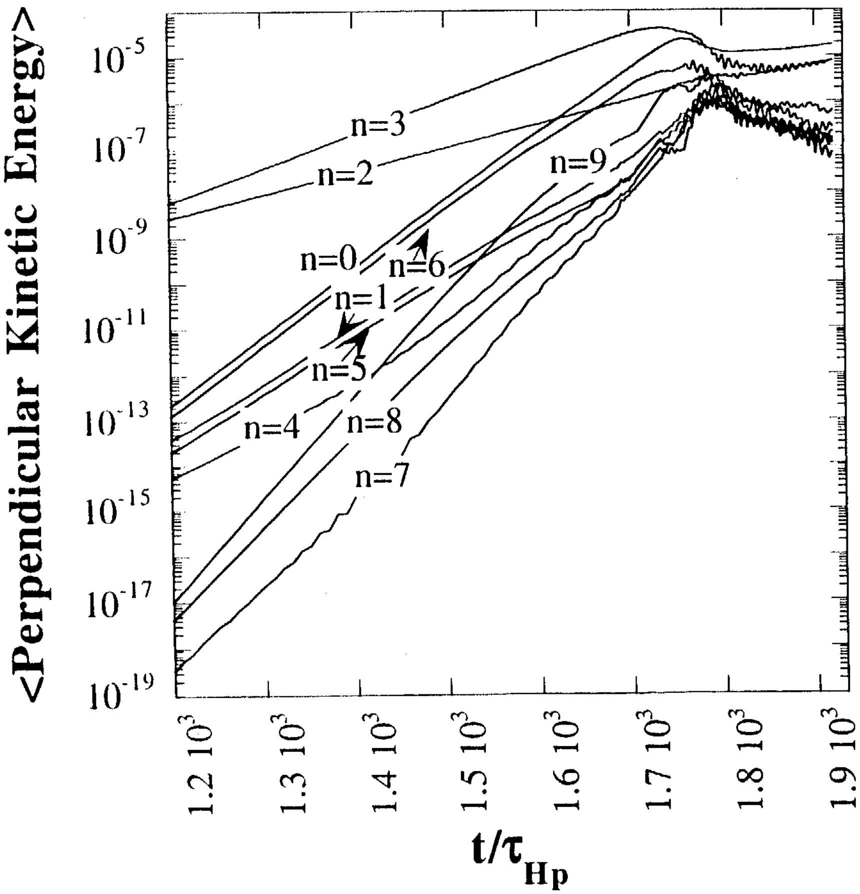

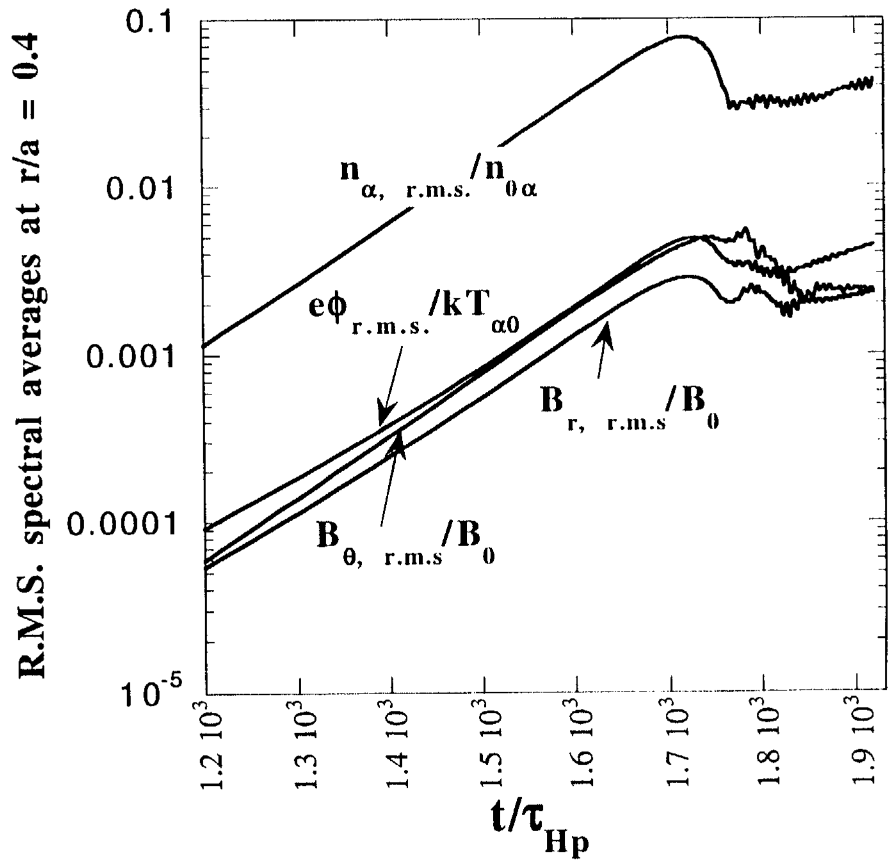

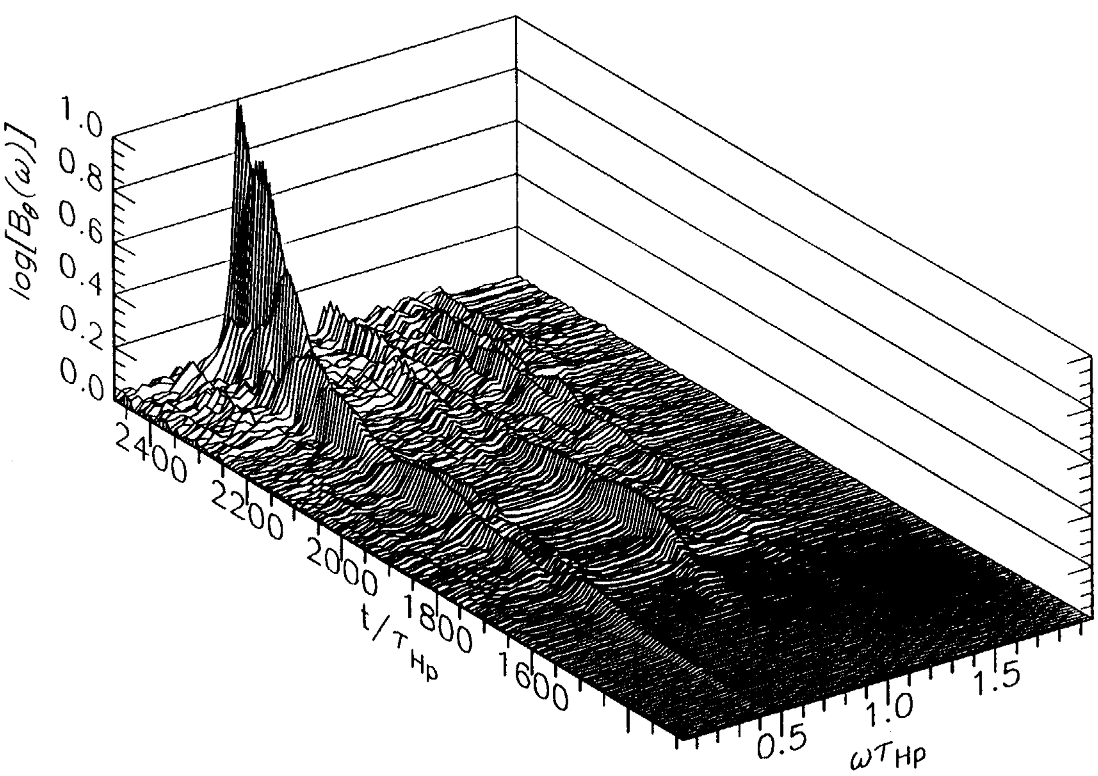

log[B_θ(ω)]
1.0
0.8
0.6
0.4
0.2
0.0
2400
2200
2000
1800
1600
t/τ_Hp
0.5
1.0
1.5
ωτ_Hp

The frequency peak for the GAE mode in the simulation is close to that observed in W7AS:

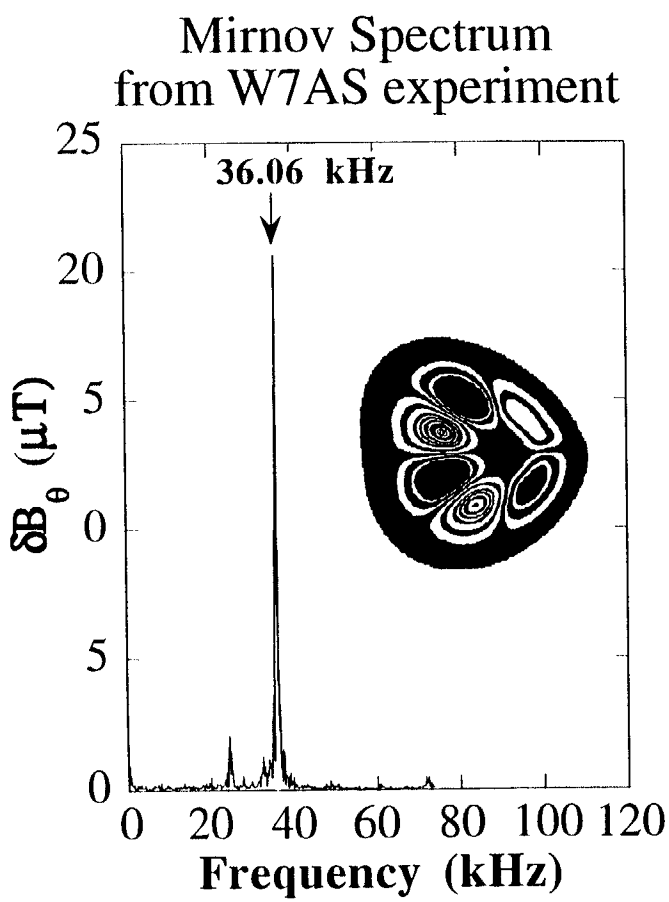

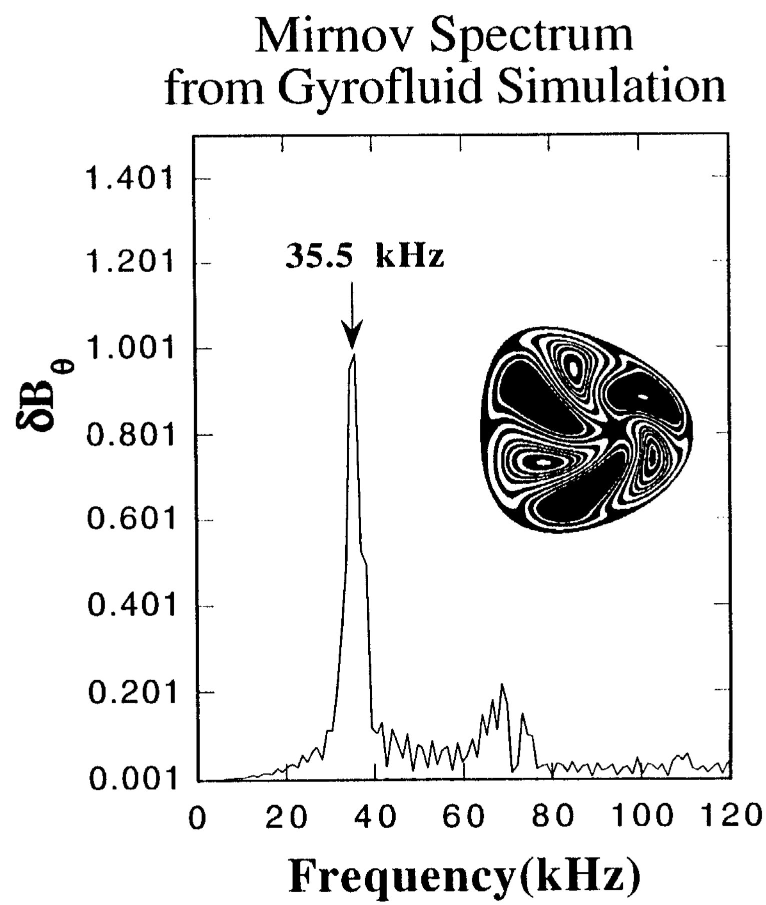

The shear velocity flow effects are generated through the vorticity equation

- **Vorticity Equation:** $$\frac{\partial U}{\partial t} = -\frac{1}{c} R\vec{B} \bullet \vec{\nabla}\left(\frac{\tilde{J}_\varphi}{B_\varphi}\right) + \left[\hat{e}_\varphi \times \vec{\nabla}\left(\frac{R}{B_\varphi}\right)\right] \bullet \vec{\nabla}\tilde{p}_\alpha + \mu\nabla_\perp^2 U$$

  where $$U = \hat{e}_\varphi \bullet \left[\vec{\nabla} \times \left(\frac{\rho_{ion} R}{B_\varphi^2} \vec{\nabla}_\perp \tilde{\phi} \times \hat{e}_\varphi\right)\right]$$

- **Flow Evolution equation (flux surface average of vorticity equation):**

$$\frac{\partial}{\partial t}\left\langle \frac{\rho_{ion} R}{B_\varphi} v_\theta \right\rangle = \left\langle \frac{R}{B_\varphi} \frac{\partial \tilde{p}_\alpha}{\partial \theta} \right\rangle - \left\langle \frac{1}{B_\varphi} J_{\varphi,eq} \frac{\partial \tilde{\psi}}{\partial \theta} \right\rangle + \left\langle U \frac{\partial \phi}{\partial \theta} \right\rangle - \left\langle \frac{\tilde{J}_\varphi}{B_\varphi} \frac{\partial \tilde{\psi}}{\partial \theta} \right\rangle + \left\langle \mu \nabla_\perp^2 U \right\rangle$$

Linear terms **unique to toroidal geometry** m > 0 equilibrium couples with n = 0, m > 0 fluctuations	**Reynold's stresses** **(nonlinear)** electrostatic and electromagnetic components	**Viscous** **Damping**

ornl

Balance of flow generation terms

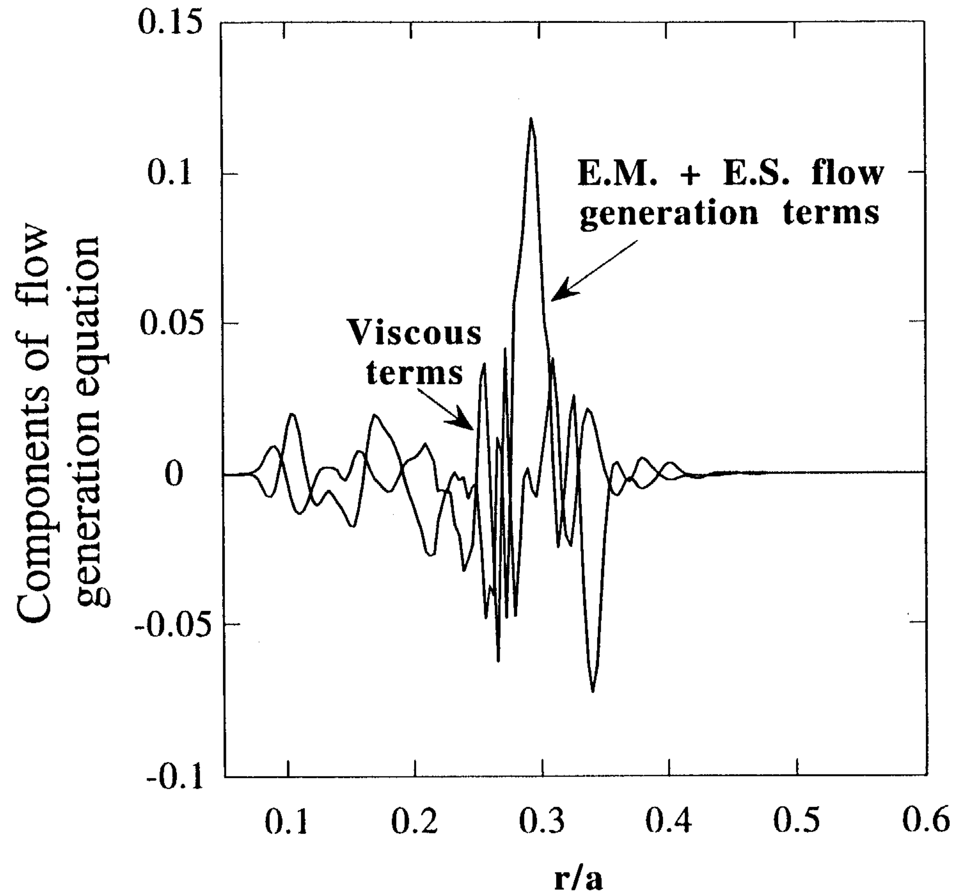

ornl

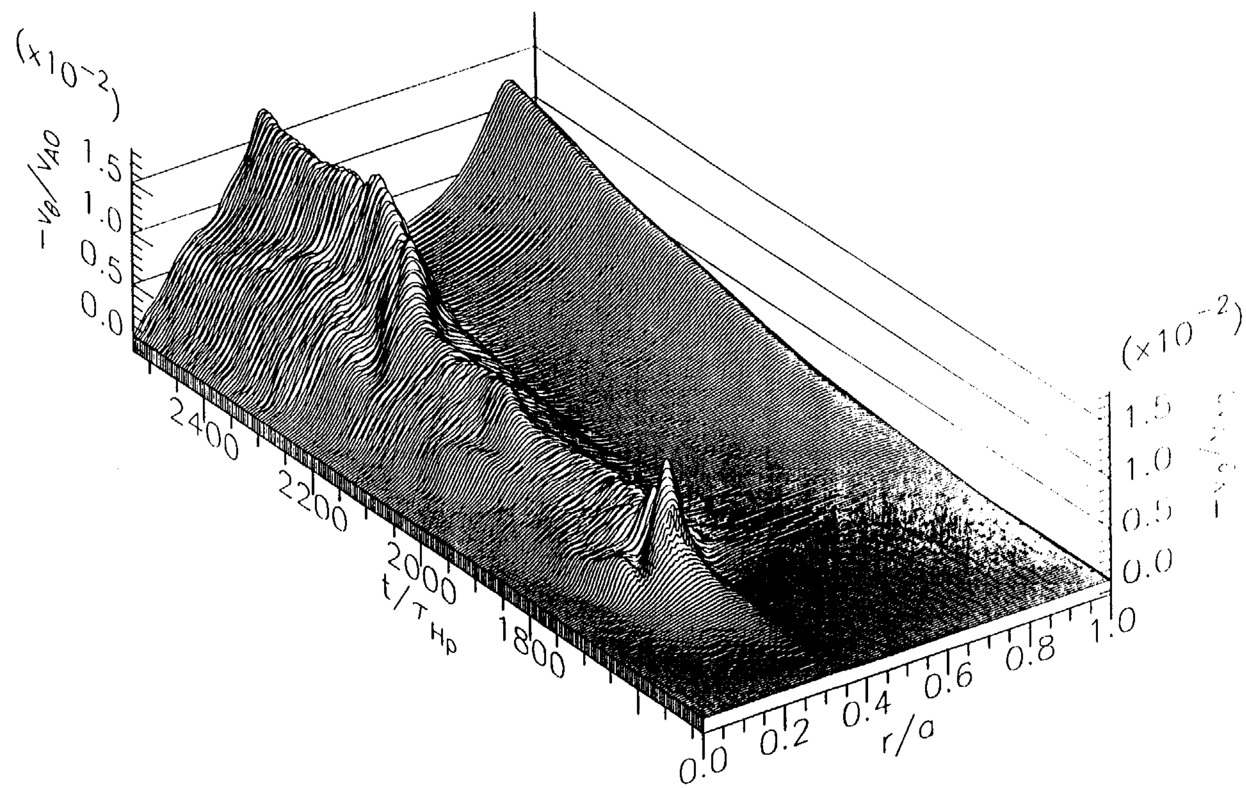

(×10⁻²)
$-v_\theta/v_{A0}$
1.5
1.0
0.5
0.0
2400
2200
2000
1800
t/τ_{Hp}
0.0
0.2
0.4
0.6
0.8
1.0
r/a
(×10⁻²)

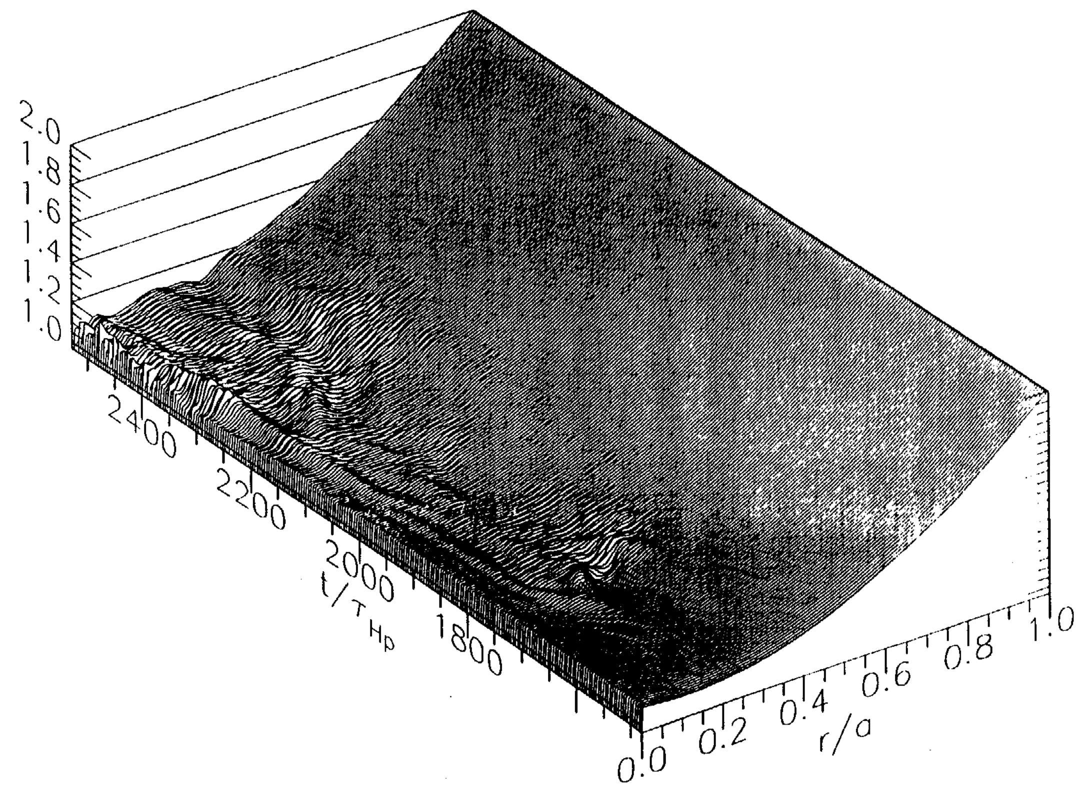

Figure 7

The maximum velocity shear is aligned with the n = 3 gap location.

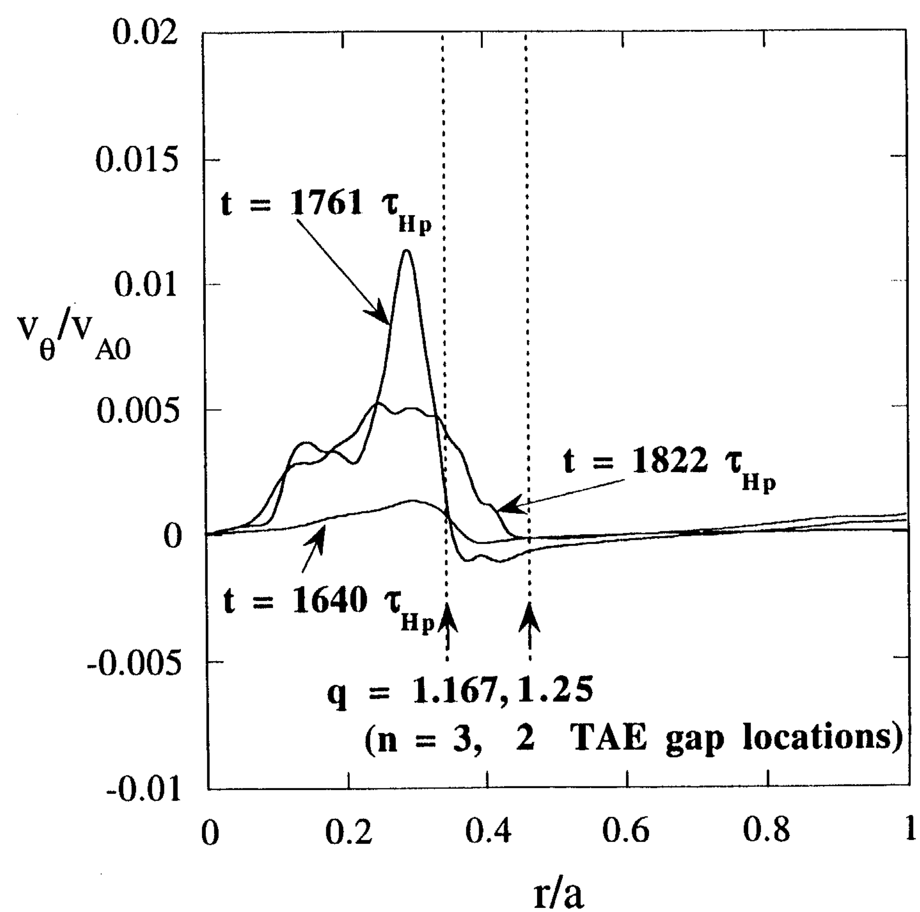

ornl

The effect of the n = 0, m = 0 components can be diagnosed by examining their effect on linear growth rates

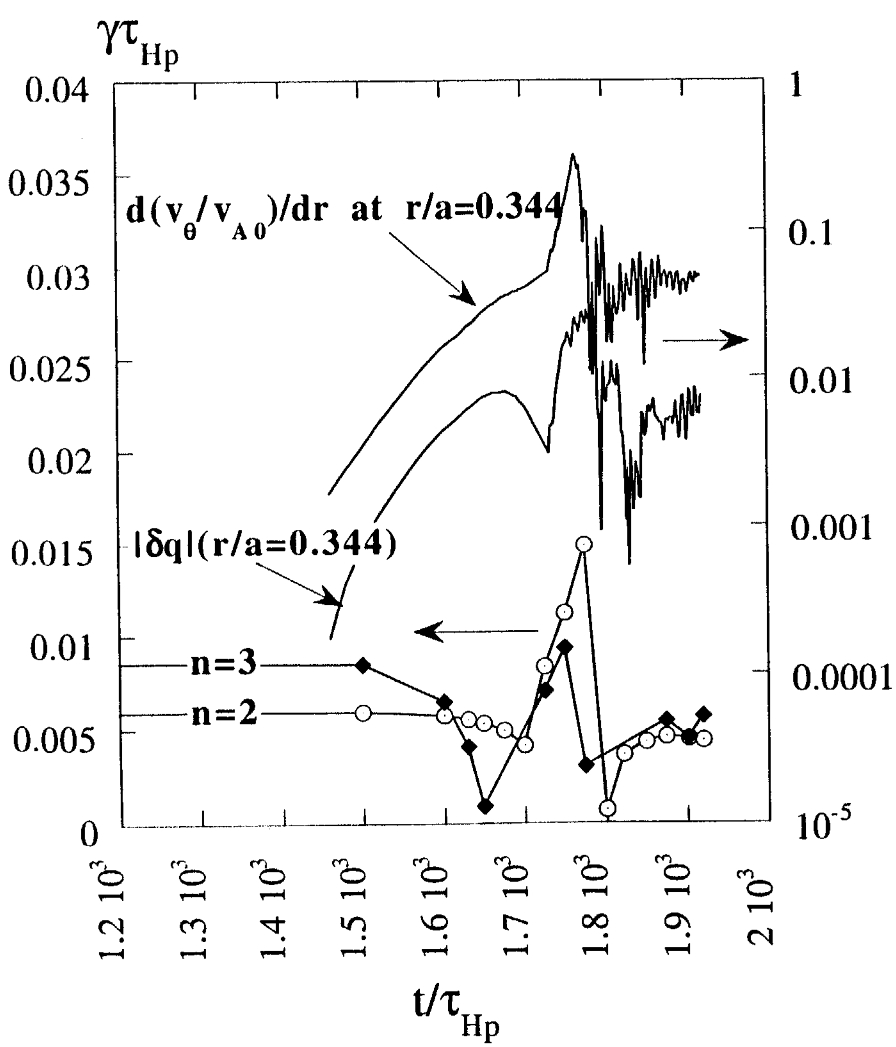

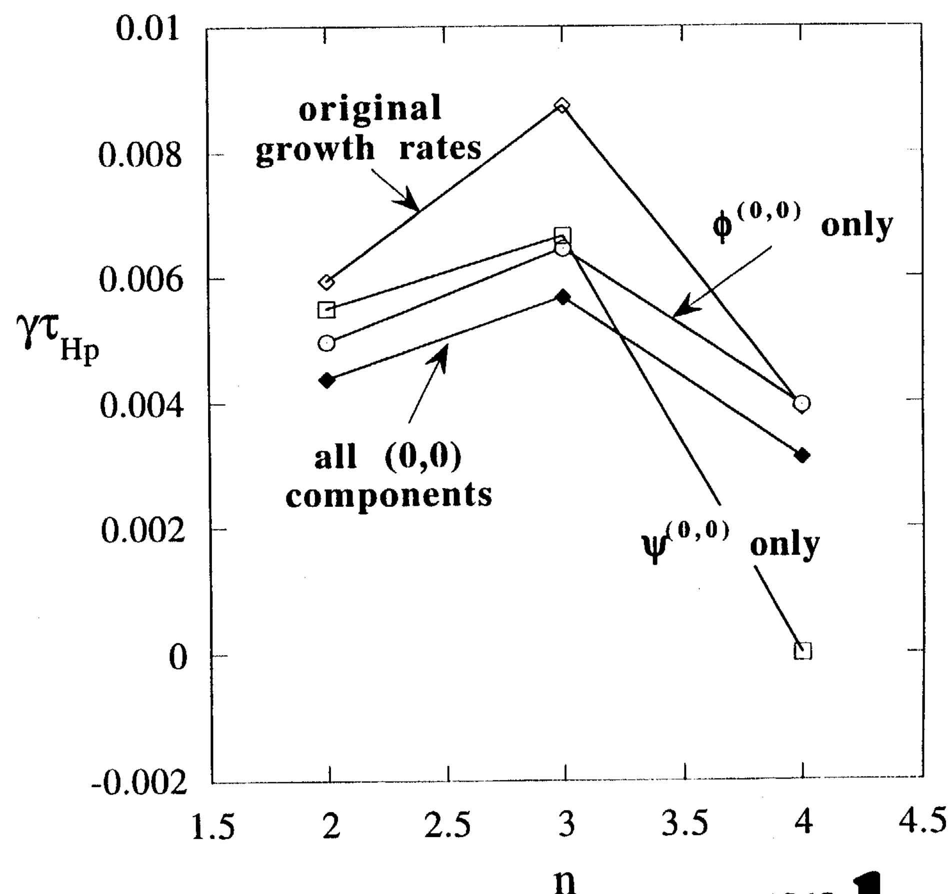

ornl

CONCLUSIONS

- **Our model is consistent with beam-driven TAE thresholds on TFTR and DIII-D**
- **TFTR-DT supershots are predicted to be stable to α-driven TAE's**
- **These thresholds can be lowered by:**
  - » Raising q(0) to around 1.5 (aligns gaps with max. dp_α/dr) (q-PROFILE CONTROL)
  - » Lowering T_{ion}, but need to maintain β_α (PELLETS, GAS PUFF)
  - » Vary v_α/v_A to enhance resonant coupling (DENSITY CONTROL)
  - » Above techniques can have future applications to He ash removal, burn control

CONCLUSIONS (Continued)

- **Our model indicates the GAE (Global Alfvén Mode) can be excited in low shear stellarators such as W7-AS**
  - » Excited for $\langle v_{fast,\,ion} \rangle / v_A \approx 0.15$ to 0.4
  - » Growth rate shows broad, but resonant peaks with rational iotas
  - » Stabilized by shear in iota profile (e.g., from increasing β)
  - » Issue for future devices: Will there be a stable window between GAE and TAE instabilities?
- **The GAE (Global Alfvén Mode) can be induced in tokamaks if q(r) is flat near the center**
  - » Of concern for TPX, ITER where high bootstrap currents cause central weak negative shear regions

CONCLUSIONS (Continued)

- **Nonlinear TAE/GAE Behavior**
  - » Simulations of edge magnetic fluctuation spectra with this model have shown similarities with experiments
  - » Nonlinear evolution is eventually dominated by the $n = 0$ component
  - » Saturation mechanisms:
    - – sheared $\vec{E}\times\vec{B}$ flow generation/amplification
    - – q-profile modification
    - – $\vec{E}\times\vec{B}$ convection of α density
  - » Observed saturation suggests: TAE/GAE's can possibly be controlled by RF generated sheared flows.